DISSERTATIONES
MATHEMATICAE
UNIVERSITATIS
TARTUENSIS
139

MOHAMMED MAINUL HOSSAIN

Numerical analysis of vibrations of nanobeams

DISSERTATIONES MATHEMATICAE UNIVERSITATIS TARTUENSIS
139

DISSERTATIONES MATHEMATICAE UNIVERSITATIS TARTUENSIS
139

MOHAMMED MAINUL HOSSAIN

Numerical analysis of vibrations of nanobeams

UNIVERSITY OF TARTU
Press
1632

Institute of Mathematics and Statistics, Faculty of Science and Technology, University of Tartu, Estonia.

Dissertation has been accepted for the commencement of the degree of Doctor of Philosophy (PhD) in Mathematics on 22 June, 2022 by the Council of the Institute of Mathematics and Statistics, University of Tartu.

Supervisor

Professor	Jaan Lellep Institute of Mathematics and Statistics University of Tartu, Estonia

Opponents

Professor	Zdeněk Kala Brno University of Technology Brno, Czech Republic
Professor	Evgeny Barkanov Riga Technical University Riga, Latvia

The public defense will take place on August 30, 2022 at 11:15 in Narva mnt 18-1008.

The publication of this dissertation was financed by the Tartu ASTRA Project PER ASPERA (European Regional Development Fund) and Institute of Mathematics and Statistics, University of Tartu.

ISSN 1024-4212
ISBN 978-9949-03-973-9 (print)
ISBN 978-9949-03-974-6 (PDF)

University of Tartu Press
http://www.tyk.ee/

CONTENTS

LIST OF ORIGINAL PUBLICATIONS

1. Mainul Hossain and Jaan Lellep, Natural vibration of axially graded multi cracked nanobeams in thermal environment using power series, J. Vib. Eng. Technol., (2022), "https://doi.org/10.1007/s42417-022-00555-3".
2. Mainul Hossain and Jaan Lellep, Analysis of free vibration of tapered cracked double nanobeams using Maclaurin series, Eng. Res. Express, **4(2)**, 025034 (2022).
3. Mainul Hossain and Jaan Lellep, Transverse vibration of tapered nanobeam with elastic supports, Eng. Res. Express, **3(1)**, 015019 (2021).
4. Mainul Hossain and Jaan Lellep, Natural vibrations of nanostrips with cracks, Acta et Com. Uni. Tartuensis De Math., **25(1)**, 87-105 (2021).
5. Mainul Hossain and Jaan Lellep, Thermo mechanical vibration of single wall carbon nanotube partially embedded into soil medium, Agron. Res., **19(1)**, 777-787 (2021).
6. Mainul Hossain and Jaan Lellep, Mode shape analysis of dynamic behaviour of cracked nanobeam on elastic foundation, Eng. Res. Express, **3(4)**, 045003 (2021).
7. Mainul Hossain and Jaan Lellep, The effect of rotatory inertia on natural frequency of cracked and stepped nanobeam, Eng. Res. Express, **2(3)**, 035009 (2020).
8. Mainul Hossain and Jaan Lellep, Effect of temperature on dynamic behavior of cracked metallic and composite beam, Vibroengineering Procedia, **32**, 172-178 (2020).
9. Jaan Lellep and Mainul Hossain, Free vibrations of rectangular nanoplate strips, The proceedings of the 13th international conference Modern Building Materials, Structures and Techniques, 743-749 (2019).
10. Mainul Hossain and Jaan Lellep, Natural vibration of stepped nanoplate with crack on an elastic foundation, IOP Conf. Ser. Mater. Sci. Eng., **660**, 012051 (2019).

Author's contribution

The author of this dissertation is responsible for majority of the research in all phases (including simulation, analysis, writing and presenting results) of the papers (1-10). The solution techniques were developed in co-operation with the supervisor; the statement of the problem belongs to the supervisor.

1. INTRODUCTION

1.1. Literature review

In recent years, researchers have been attracted by nanomaterials due to their exceptional properties and unavoidable roles in modern science and technology. These exceptional characteristics distinguish nanomaterials from their bulk counterparts. Nanomaterials consist of a larger surface volume ratio than macromaterials. An increase in surface volume ratio increases the number of surface atoms. These surface atoms have unsatisfied bonds that make nanomaterials more reactive than their bulk counterparts (see Li and Wang [45], Li et al. [49]). That is why, nanomaterials possess some strange and vital characteristics such as high strength, high stiffness, and excellent thermal and electrical conductivities (see Abid et al. [1]).

During the application, the nanomaterials are subjected to various forces such as compression, tension, and vibration. In order to overcome the adverse effects of these forces, effective modeling is essential. Several techniques are involved to investigate the behavior of nano-structure such as molecular dynamics simulation, and numerical methods. Among them, the numerical technique is cost-effective, easy to handle, and a widely accepted technique among researchers (Pham et al. [61]). However, the existing continuum theory is not adequate for numerical analysis because it cannot incorporate the small-scale effect (Adhikari et al. [2], Ahmadi [4]). Researchers introduce the gradient theories of continuum mechanics to analyze the nano-devices and to encounter the size effect (Faghidian [21]). Basically, there are two types of gradient theories such as the strain and the stress gradient theories of elasticity that are engaged to analyze nanomaterials (Faghidian [22], Karami and Janghorban [40]). Generally, the stress gradient theory is proposed on the basis of an integro-differential equation whose solution is difficult. That is why Eringen (see Eringen [18]) proposed equivalent differential nonlocal elasticity theory which has been widely accepted to analyze nanomaterials.

Research on nanobeams has started in the recent decade. Researchers have engaged in this research profoundly to explore the behavior of nanobeams. Here, the contributions of some authors studying nanobeams are presented briefly. First of all, the nonlocal Euler–Bernoulli beam was investigated by Eltaher et al. [16] using the finite element method. They presented the efficiency of the model to analyze nanobars, nanotubes, and nanobeams. In another paper, Eltaher et al. [17] described the coupling effects of the nonlocal parameter and surface energy on vibration analysis of nanobeams. They revealed that the surface properties had significant effects on the fundamental frequency in nano and micro-structures. In addition, free vibration of the nonlocal beam was presented by Ke and Wang [41]. They described the effects of electric potential, magnetic potential, and temperature rise. Their results revealed that the electric and magnetic loadings had significant effects on the natural frequency of nanobeams. After that, Simsek [70]

analyzed the free vibration of nanobeams with large amplitude. He examined the effect of the nonlocal parameter on the nonlinear frequency ratio. His model produced a larger nonlinear frequency ratio than the classical (local) beam model.

Ahmadvand and Asadi [5], Chinka et al. [11], Kala [38], Kumar and Singh [42], Rosa and Lippiello [67], Sushobhan and Khazanovich [75] studied the crack as a newly generated surface that partially separated the intact body or structure. During the formation of a crack, the surface area is created in the material in a thermodynamically irreversible manner. The crack is created due to environmental corrosion, operational condition, inappropriate loading, etc. Natural frequency is significantly affected by crack location and cracks severity (Eroglu and Tufekci [19]). The mode shape of the vibration of nanomaterials is significantly changed by the presence of cracks (Hossain and Lellep [34], Song et al. [72], Wu et al. [78]).

After analyzing the nanobeam, several authors showed their interest in cracked nanobeams. First of all, Hashemi et al. [23] explored the dynamic behavior of thin and thick cracked nanobeams with surface effects. Their results illustrated that the surface effects on natural frequencies depended on the length of nanobeams. On the other hand, the effects of cracks on natural vibration did not depend on the length of nanobeams. In addition, the longitudinal vibration of cracked nanobeams was scrutinized by Hsu [37]. This analysis showed that the increase of nonlocal parameters decreased the effect of cracks on the natural frequency. Similarly, Roostai and Haghpanahi [66] considered the vibration of nanobeams with multiple cracks. They observed the effects of crack locations and parameters on the vibration of nanobeams. After that, Hasheminejad et al. [24] explained the dynamic behavior of cracked nanobeams with surface effects. Moreover, Aria et al. [6] demonstrated the vibration of cracked nanobeams on elastic matrix. They observed the effects of crack severity, crack location, and temperature on the natural frequency of nanobeams. Moreover, Bahrami [8] applied a wave-based method to analyze cracked nanobeams. It was shown in [8] that the natural frequency decreased with the increase of the nonlocal parameter. Whereas, in a cantilever beam, the natural frequency increased with the increase of the nonlocal parameter. The free vibration of multi-cracked and stepped nonlocal nanobeams was studied by Loghmani and Yazdi [51]. They observed that the crack had no impact on frequency when it was located at the inflection points of the mode shape.

The advanced manufacturing process overcomes the difficulties to fabricate the non-prismatic beams consisting of complex cross-sections (Ece et al. [15], Yan et al. [79], Zhang et al. [81]). Stepped (see Lellep and Lenbaum [43], Lellep and Lenbaum [44]), tapered, sandwich (see Barkanov [9]) and axially graded beams (Li et al. [48], Mamaghani et al. [55], Rajasekaran and Khaniki [64]) are the forms for optimal design to improve the performance of structures (Karami and Janghorban [40]). Due to the reasonable choice of dimension, the stepped beam is economical because it provides a larger cross-section along the critical segment

instead of all over the span. Stepped beams under vibration load face complex excitation that may be the cause of failure. It is essential to develop a reliable model to study stepped beams under vibration (Afefy et al. [3], Ni and Hua [59], Šalinić et al. [68], Su et al. [73], Surla et al. [74]). In addition, a tapered beam is preferable to the designer because of its cost-effective and material-saving properties (see Chockalingam et al. [12], Chockalingam et al. [13], Prasad and Banerjee [62], Rajasekaran and Khaniki [63], Wan et al. [77]). There is no abrupt change in cross-section or geometric properties as well as there is no stress concentration or fatigue failure. Moreover, an axially graded beam (Datta [14], Li et al. [47], Šalinić et al. [68], Zhang et al. [82]) is a type of composite where the material properties differ smoothly from one end to another end for eliminating the stress concentration at any specific cross-section. The axially functionally graded material is one of the exceptional innovations of recent science and technology that satisfies the growing demand for advanced materials having exceptional properties for high-quality design.

Solution techniques are essential for proper analysis. Some solution techniques have been presented in this study where these techniques are rare in the existing literature to analyze the nano-structures. The homotopy perturbation method, power series, and Maclaurin series are used in this research. First of all, the homotopy perturbation method developed by He (see He [25-27]) is a useful technique for analyzing nonlinear problems. It is the combination of homotopy analysis and perturbation technique where it overcomes the limitations of the conventional perturbation method. In addition, the power series solution technique (see Soltani et al. [71]) is also used for analyzing the differential equations. Basically, the power series is an infinite series. Any polynomial can be expressed as a power series around a certain point. Moreover, the Maclaurin series is a semi-analytical technique based on the Taylor series. Generally, the Maclaurin series is a special form of the Taylor series where the derivatives are calculated at the initial position. All these above techniques have been successfully employed during this analysis.

1.2. Aim of the dissertation

The aim of the dissertation is to analyze the dynamic behavior of nanobeams with different physical and geometrical properties using semi-analytical and numerical techniques. Euler-Bernoulli beam theory and Eringen's nonlocal theory of elasticity are applied to derive the governing equations of nanobeams. Cracks, steps, and taper ratios are considered as geometric irregularities. On the other hand, axially graded material, and surrounding temperature are considered as physical properties.

The significant feature of this analysis is the solution techniques. Several techniques such as homotopy perturbation method, power series, and Maclaurin series are employed in this analysis. These techniques are rare to analyze the nanomaterial. These techniques have been employed effectively in this analysis and ob-

tained results are compared with the results of other researchers in the existing literature.

1.3. Structure of the dissertation

The dissertation is organized as follows. Section 1 contains the literature review for the nanobeam with different physical and geometrical properties. In section 2, some essential theories, different physical and geometrical properties, and some numerical techniques are presented briefly. In section 3, the effects of rotatory inertia on the natural frequency of nanobeams with steps and cracks are presented. The exact solution technique and homotopy perturbation method are applied for this analysis. In section 4, the dynamic behavior of cracked tapered double nanobeams is analyzed using the Maclaurin series solution technique. In section 5, the transverse vibration of tapered nanobeams with elastic supports is demonstrated. The homotopy perturbation method is used to solve this problem. In section 6, the analysis of the natural frequency of axially graded multi-cracked nanobeams in a thermal environment is presented. The power series solution technique is applied for this analysis. Finally, concluding remarks are presented at the end of the dissertation.

2. GOVERNING EQUATIONS AND ASSUMPTIONS

2.1. Nonlocal theory

Accurate analysis is essential for nanomaterials to utilize their exceptional properties effectively. However, the conventional continuum theory is unable to compute the mechanical behavior of nano-scale materials because it cannot incorporate the size effects of nanomaterials. To overcome the limitations of the existing continuum theory, Eringen [18] proposed the nonlocal theory of elasticity based on assumptions that the stress at a point depends on the strain of all points of the continuum rather than on that point only. According to the assumption, the stress-strain relationship (see Atanasov and Stojanovic [7], Cardoso [10], Malik and Das [54], Martin and Salehian [57]) for a three-dimensional isotropic elastic solid can be expressed as

$$\sigma_{ij}(x) = \int_V f_c(\mid x - x' \mid, \tau) t_{ij}(x') dV(x'), \tag{2.1}$$

where

$$t_{ij}(x') = \psi \varepsilon_{rr}(x') \delta_{ij} + 2\phi \varepsilon_{ij}(x'). \tag{2.2}$$

Here ψ and ϕ represent Lame's constants. Here $t_{ij}(x')$ and $\varepsilon_{ij}(x')$ are the classical stress tensor and linear strain tensor at any point x' in the body, respectively. According to the Hooke's law, the stress-strain relationship can be expressed as

$$t_{ij} = C_{ijkl} \varepsilon_{kl}, \tag{2.3}$$

where C_{ijkl} denotes the elastic constants. In equation (2.1), $f_c(\mid x - x' \mid, \tau)$ represents the nonlocal modulus to indicate the nonlocal effects into the constitutive equation for the reference point x and source point x', respectively. Here, $\mid x' - x \mid$ represents the Euclidean distance and τ can be presented as

$$\tau = \frac{e_0 a_0}{l}. \tag{2.4}$$

Here τ is a constant that indicates the ratio of internal and external characteristic lengths of the nanomaterial, where e_0 is the material constant. According to the theory of nonlocal elasticity, the integral constitutive relations can be transformed into the equivalent differential equation by substituting the kernel $f_c(\mid x' - x \mid, \tau)$ as below

$$(1 - (e_0 a_0)^2 \Delta^2) \sigma_{kl} = t_{kl}. \tag{2.5}$$

In (2.5), Δ^2 denotes the Laplacian operator, σ_{kl}, t_{kl} are the nonlocal and classical stress, respectively. The nonlocal theory depends on the internal characteristic length a_0. When a_0 becomes zero, the nonlocal constitutive relationship transforms into the classical theory of elasticity. In the one dimensional case, the nonlocal stress-strain relationship can be presented as

$$\sigma(x) - (e_0 a_0)^2 \frac{\partial^2 \sigma(x)}{\partial x^2} = E \varepsilon(x), \tag{2.6}$$

where $\sigma(x)$ and $\varepsilon(x)$ represent the stress and strain along the x-axis, E is the modulus of the elasticity. Therefore, the nonlocal elasticity theory can be presented in terms of bending moment M, as follows

$$M-(e_0a_0)^2\frac{\partial^2 M}{\partial x^2}=EI(-\frac{\partial^2 W}{\partial x^2}), \tag{2.7}$$

where W is the deflection of the beam, I indicates the area moment of inertia. According to the nonlocal theory, the equation (2.7) represents the relationship between the bending moment and the deflection.

2.2. Euler-Bernoulli theory

Euler-Bernoulli beam theory is widely used in research and engineering. This theory considers axial and flexural deformation, while the shear deformation is neglected. According to the Euler-Bernoulli's theory, the displacement fields can be expressed as (Malik et al. [53], Yin et al. [80])

$$\begin{aligned} U_1(x,z,t)&=U(x,t)-z\frac{\partial W(x,t)}{\partial x},\\ U_2(x,z,t)&=0,\\ U_3(x,z,t)&=W(x,t), \end{aligned} \tag{2.8}$$

where U_1, U_2, U_3 express the deflection in x, y and z axis respectively, t indicates the time, $W(x,t)$ and $U(x,t)$ define the transverse and axial deflection, respectively. One can write the axial strain as

$$\varepsilon_{xx}=\frac{\partial U}{\partial x}-z\frac{\partial^2 W}{\partial x^2}. \tag{2.9}$$

Considering the axial load N and moment M, the Euler-Bernoulli equation for vibration can be presented as

$$\frac{\partial^2 M}{\partial x^2}+\frac{\partial}{\partial x}(N\frac{\partial W}{\partial x})-m_0\frac{\partial^2 W}{\partial t^2}=0, \tag{2.10}$$

where $m_0=\rho A$ is the mass per unit length.

2.2.1. Transform functions

Basically, the equation of motion is a partial differential equation. Therefore, this partial differential equation can be transformed into an ordinary differential equation using the following function

$$W(x,t)=\bar{W}(x)e^{i\omega_c t}, \tag{2.11}$$

here ω_c is the dimensional frequency.

2.2.2. Non-dimensional parameters

For dimensionless analysis, non-dimensional parameters are essential. Some of the dimensionless parameters are included as follows

$$\xi = \frac{x}{L},\ w = \frac{\bar{W}}{L},\ \mu = \frac{e_0 a_0}{L},\ n = \frac{NL^4}{EI},\ \omega^2 = \bar{\omega}^4 = {\omega_c}^2 L^4 \frac{A\rho}{EI}, \tag{2.12}$$

where ρ is the density of the material, L represents the length of the beam, A stands for the area of the section, I is the moment of inertia of this section, N denotes the axial load and ω_c is the dimensional frequency of natural vibration.

2.2.3. Boundary conditions

To solve the Euler-Bernoulli equation, the required boundary conditions in terms of deflection (W) and moment (M) can be written as follows

for simply supported ends (SS)

$$W(0) = 0, \quad M(0) = 0, \quad W(L) = 0, \quad M(L) = 0, \tag{2.13}$$

for clamped ends (CC)

$$W(0) = 0, \quad W'(0) = 0, \quad W(L) = 0, \quad W'(L) = 0, \tag{2.14}$$

in the case of clamped at the left and simply supported at the right ends (CS)

$$W(0) = 0, \quad W'(0) = 0, \quad W(L) = 0, \quad M(L) = 0, \tag{2.15}$$

for cantilever beams (CF)

$$W(0) = 0, \quad W'(0) = 0, \quad M(L) = 0, \quad M'(L) = \mu^2 \omega^2 W'(L). \tag{2.16}$$

2.3. Modeling of cracks

The basic theory for elastic cracks was established in 1921 by Griffith. According to his theory, crack propagation will occur if the energy is sufficient to provide all the energy that is required for crack growth. The mechanical properties of open and stable cracks can be analyzed using the classical local stiffness model. According to the model, the beam is separated into two sub-beams for each crack at the crack position. The stiffness of the rotational spring depends on strain energy release rate as well as the crack depth. The strain energy S of the cracked beam in terms of axial force and bending moment can be expressed as

$$S = \frac{1}{2} \int_0^L \left(N \frac{\partial U}{\partial x} + M \frac{\partial^2 W}{\partial x^2} \right) dx + \Delta s_c. \tag{2.17}$$

Due to the presence of a crack, the beam has additional strain energy to the rotational spring. Strain energy is caused by the bending moment and axial stress. The change of strain energy (Roostai and Haghpanahi [66]) can be presented as

$$\Delta s_c = \frac{1}{2} M \Delta\theta + \frac{1}{2} N \Delta u, \tag{2.18}$$

where $\Delta\theta$ indicates the rotational angle because of the spring and Δu represents the axial displacement at the location of the crack. Therefore, these can be expressed as

$$\begin{aligned} \Delta\theta &= K_{MM} \frac{\partial^2 W}{\partial x^2} + K_{MN} \frac{\partial U}{\partial x}, \\ \Delta u &= K_{NN} \frac{\partial U}{\partial x} + K_{NM} \frac{\partial^2 W}{\partial x^2}, \end{aligned} \tag{2.19}$$

where K_{MM}, K_{MN}, K_{NN}, K_{NM} are the flexibility constants. When the beam is subjected to transverse vibration, longitudinal displacement Δu and the flexibility constants K_{MN}, K_{NN}, K_{NM} are small which can be neglected. Therefore, the discontinuity at the location of the crack can be expressed as

$$\Delta\theta = \frac{K_{MM}}{L} \frac{\partial^2 W(x)}{\partial x^2} \mid_{x=a}, \tag{2.20}$$

where $\frac{K_{MM}}{L}$ can be replaced by K as

$$\Delta\theta = K \frac{\partial^2 W(x)}{\partial x^2} \mid_{x=a}, \tag{2.21}$$

here K is the crack severity. The crack severity depends on the crack depth and rotational spring stiffness. It can be expressed as follows

$$K = \frac{EI}{L} \frac{1}{\kappa_s}. \tag{2.22}$$

Here κ_s is the spring stiffness. It can be written as

$$\kappa_s = \frac{EI}{h} \frac{1}{C(s)}, \tag{2.23}$$

here $s = \frac{c}{h}$ is the ratio of crack depth (c) and beam height (h). In (2.23), $C(s)$ is the local compliance that can be computed from the strain energy density function as

$$\begin{aligned} C(s) = 5.346(&1.86s^2 - 3.95s^3 + 16.375s^4 - 37.226s^5 + 76.81s^6 \\ &-126.9s^7 + 172s^8 - 143.97s^9 + 66.56s^{10}). \end{aligned} \tag{2.24}$$

The crack severity can be written according to equations (2.22) and (2.23) as

$$K = \frac{h}{L} C(s). \tag{2.25}$$

Crack severity doesn't depend on the modulus of elasticity and density of the beam. Therefore, crack severity K is constant over the length of the axially graded beam. Another way, it can be presented (see Hsu [37]) as

$$K = \frac{6(1-\nu^2)h}{EI} f(s), \tag{2.26}$$

where

$$f(s) = \int_0^s \pi s F^2(s) ds, \tag{2.27}$$

and ν is the Poisson ratio. The factor F can be defined by trigonometric or algebraic functions (see Tada [76]) as

$$F(s) = \sqrt{\frac{2}{\pi s} tan\left(\frac{\pi s}{2}\right)} \frac{0.923 + 0.199[1 - sin\left(\frac{\pi s}{2}\right)]^4}{cos\left(\frac{\pi s}{2}\right)}, \tag{2.28}$$

and

$$F(s) = 1.93 - 3.07s + 14.53s^2 - 25.11s^3 + 25.8s^4, \tag{2.29}$$

where

$$s = \frac{c}{h}. \tag{2.30}$$

Intermediate conditions for steps and cracks are as follows

$$\begin{aligned} w_i(x_i) &= w_{i+1}(x_i), \\ w_i''(x_i) &= w_{i+1}''(x_i), \\ w_{i+1}'(x_i) - w_i'(x_i) &= K w_i''(x_i), \\ w_i'''(x_i) + \psi_i w_i'(x_i) &= w_{i+1}'''(x_i) + \psi_{i+1} w_{i+1}'(x_i), \end{aligned} \tag{2.31}$$

where $\psi = \omega^2 \mu^2$.

2.4. Tapered beams

Tapered beams offer us an optimized design by saving material consumption. In this dissertation, the beam is tapered along the x-axis where the width of the beam is varying exponentially from one end to another end. The variable quantities such as width, area, moment of inertia can be expressed as (see Hossain and Lellep [32], Kalkowski et al. [39], Mahmoud [52])

$$\begin{aligned} b(x) &= b_0 e^{\alpha \frac{x}{L}}, \\ A(x) &= A_0 e^{\alpha \frac{x}{L}}, \\ I(x) &= I_0 e^{\alpha \frac{x}{L}}, \end{aligned} \tag{2.32}$$

where α is the taper ratio of the beam, it indicates the variation of width along the x-axis and b_0, A_0, I_0 are the width, area, moment of inertia at $x = 0$, respectively. The area and area moment of inertia are also varying with the width of the beam.

2.5. Axially graded beams

An axially graded beam is a non-homogeneous beam. It is also a type of composite (Li and Liu [46]) that can avoid the point of stress concentration. It distributes stress gradually from one end to another end. Along the cross-section, material properties are constant. It is assumed that the modulus of elasticity E and density ρ are varying along the length exponentially (Mamaghani et al. [55]). These can be expressed as

$$E(x) = E_0 e^{\lambda \frac{x}{L}}, \quad \rho(x) = \rho_0 e^{\lambda \frac{x}{L}}, \tag{2.33}$$

where E_0 and ρ_0 are the modulus of elasticity and density at the point $x = 0$, λ is the coefficient of non-homogeneity.

2.6. Thermal loading

The thermal load is the result of temperature change which is induced by the contraction and expansion of the material. This load acts as an axial load on the beam element. Thermal load can be expressed as

$$N = -EA\alpha_t\theta, \tag{2.34}$$

where α_t is the coefficient of thermal expansion, θ is the temperature change and A stands for the area of the cross-section. According to the theory of Zarzycki 1982 and Kittel 1983, the coefficient of thermal expansion can be presented as

$$\alpha_t = \frac{\gamma_G \rho c_v}{3E}, \tag{2.35}$$

where γ_G is the Grüneisen constant and c_v stands for the specific heat of the material. Here, α_t depends on density and modulus of elasticity. Here, in the axially graded beam, both of these parameters are varying equally along the x-axis. Therefore, α_t is constant over the length.

2.7. Homotopy perturbation method

The homotopy perturbation method is a very useful technique to analyze linear and nonlinear problems. He (see He [25-27]) proposed this method in 1998. The homotopy perturbation method is the combination of the perturbation method and homotopy method. In this method, small parameters are not essential. An early approximation can be selected freely with possible unknown constants. Finally, the obtained approximations are valid for small parameters as well as very large parameters. Applying the homotopy perturbation method for solving nonlinear differential equations, one can consider the following nonlinear differential equation

$$D(w) - f(r) = 0 \quad (r \in \Omega), \tag{2.36}$$

and boundary conditions can be described as follows

$$B(w, \frac{\partial w}{\partial \xi}) = 0 \quad (r \in \Gamma), \tag{2.37}$$

where D is a general differential operator, B is a boundary operator, $f(r)$ is a known analytical function, Γ is the boundary of the solution domain (Ω), and $\frac{\partial w}{\partial \xi}$ denotes differential along the outward normal to Γ. Basically, the operator D can be divided into two parts, a linear part L and a nonlinear one N. Therefore, the equation (2.36) can be written as follows

$$L(w) + N(w) - f(r) = 0. \tag{2.38}$$

In cases where the nonlinear equation (2.38) includes no small parameter, one can construct the following homotopy equation

$$H(w, P) = L(w) + P[N(w) - f(r)] = 0. \tag{2.39}$$

In the equation (2.39), $P \in [0, 1]$ is the embedded parameter and w_0 is the first approximation that satisfies the boundary condition. One may assume that solution of the equation (2.39) can be written as a power series of P, as given below

$$w = w_0 + Pw_1 + P^2 w_2 + \ldots \quad . \tag{2.40}$$

Considering $P = 1$, equation (2.40) can be written as

$$w = w_0 + w_1 + w_2 + \ldots \quad . \tag{2.41}$$

Using the given fourth order differential governing equation (nano elements), one can calculate the first term of the series as follows

$$w_0 = B_0 + B_1 \xi + \frac{1}{2} B_2 \xi^2 + \frac{1}{6} B_3 \xi^3, \tag{2.42}$$

here, B_0, ..., B_3 are constant coefficients of the series. Similarly, one can calculate the other terms $(w_1, w_2, \ldots, w_n)$ of the series. Therefore, using the boundary conditions, the series solution can be transformed into matrix form as follows

$$[M] \begin{bmatrix} B_0 \\ B_1 \\ B_2 \\ B_3 \end{bmatrix} = 0. \tag{2.43}$$

Solving this linear algebraic equation, one can get the non-trivial solution for the governing equation.

2.8. Maclaurin series

Maclaurin series is a special case of a Taylor series around $x_0 = 0$. This series represents the approximate solution of a function $f(x)$. Therefore, this series can be expressed as

$$f(x) = \sum_{n=0}^{\infty} \frac{f^{(n)}(0)}{n!} x^n = f(0) + f'(0)x + \frac{f''(0)}{2!}x^2 + ... + \frac{f^{(k)}(0)}{k!}x^k + ..., \quad (2.44)$$

it can be considered as follows

$$\begin{aligned} f(0) &= C_0, \\ f'(0) &= C_1, \\ f''(0) &= C_2, \\ f'''(0) &= C_3. \end{aligned} \quad (2.45)$$

Similarly, using the given governing equation $f^4(0)$, $f^5(0)$, ..., $f^n(0)$ can be presented by the constants $(C_0, C_1, ..., C_3)$, then the solution becomes

$$f(x) = C_0 + C_1 x + C_2 \frac{x^2}{2} + C_3 \frac{x^3}{6} + ... \quad . \quad (2.46)$$

Using the boundary conditions, solution (2.46) can be transformed into matrix form as follows

$$[M] \begin{bmatrix} C_0 \\ C_1 \\ C_2 \\ C_3 \end{bmatrix} = 0. \quad (2.47)$$

Solving the equation (2.47), one can find the non-trivial solution.

2.9. Power series

The power series solution (Soltani et al. [71]) is a semi-analytical technique. In this technique, a power series is considered as a solution of the function. Therefore, the differential equation transforms into an algebraic equation. Linear and nonlinear differential equations can be solved using the power series solution technique. Let us consider a series for the deflection of the beam as

$$w = \sum_{k=0}^{\infty} A_k \xi^k, \quad (2.48)$$

here, A_k represent the constant coefficients of the series. Similarly, derivatives of deflection can be written as

$$\begin{aligned}
\frac{dw}{d\xi} &= \sum_{k=1}^{\infty} kA_k\xi^{k-1}, \\
\frac{d^2w}{d\xi^2} &= \sum_{k=2}^{\infty} k(k-1)A_k\xi^{k-2}, \\
\frac{d^3w}{d\xi^3} &= \sum_{k=3}^{\infty} k(k-1)(k-2)A_k\xi^{k-3}, \\
\frac{d^4w}{d\xi^4} &= \sum_{k=4}^{\infty} k(k-1)(k-2)(k-3)A_k\xi^{k-4}.
\end{aligned} \tag{2.49}$$

Using the governing equation, it is needed to make a recursive relationship between coefficients as follows

$$A_{k+4} = g_1A_{k+3} + g_2A_{k+2} + g_3A_{k+1} + g_4A_k, \tag{2.50}$$

here, g_1, ..., g_4 are the constants come from the given governing equation. Applying this relationship, one can calculate $A_4, A_5, A_6, ..., A_n$ in terms of $A_0, A_1, ..., A_3$. Therefore, one can write the series solution as follows

$$w = A_0 + A_1\xi + A_2\xi^2 + A_3\xi^3 + ... \quad . \tag{2.51}$$

Using the boundary conditions, this series solution can be transformed into matrix form as below

$$[M]\begin{bmatrix} A_0 \\ A_1 \\ A_2 \\ A_3 \end{bmatrix} = 0. \tag{2.52}$$

Solving this equation, one can get the non-trivial solution.

3. THE EFFECT OF ROTATORY INERTIA ON THE NATURAL FREQUENCY OF CRACKED AND STEPPED NANOBEAMS

In this section, the effect of rotatory inertia is considered in the analysis of the dynamic behavior of the cracked and stepped nanobeams. Usually, in the Euler-Bernoulli beam theory, the effect of rotatory inertia is ignored. Here, it is taken into account. In this section, the Euler-Bernoulli beam theory combined with rotatory inertia is solved using two techniques such as the exact solution method in Hossain and Lellep [28, 29] and the homotopy perturbation method in Hossain and Lellep [33].

3.1. Formulation of the problem

A schematic shape of a stepped and cracked nanobeams is illustrated in Figure 1. It is assumed that the origin of the coordinate system is placed at the left corner point of the nanobeam. The axis of the beam coincides with the x-axis and the height of the beam along the z-axis. The nanobeam with length L and rectangular cross-section of width b is considered. The density of the material ρ is constant throughout the beam and the axial load N is also applied uniformly over the nanobeam. The crack and step are placed at the same location at $x = a$ of

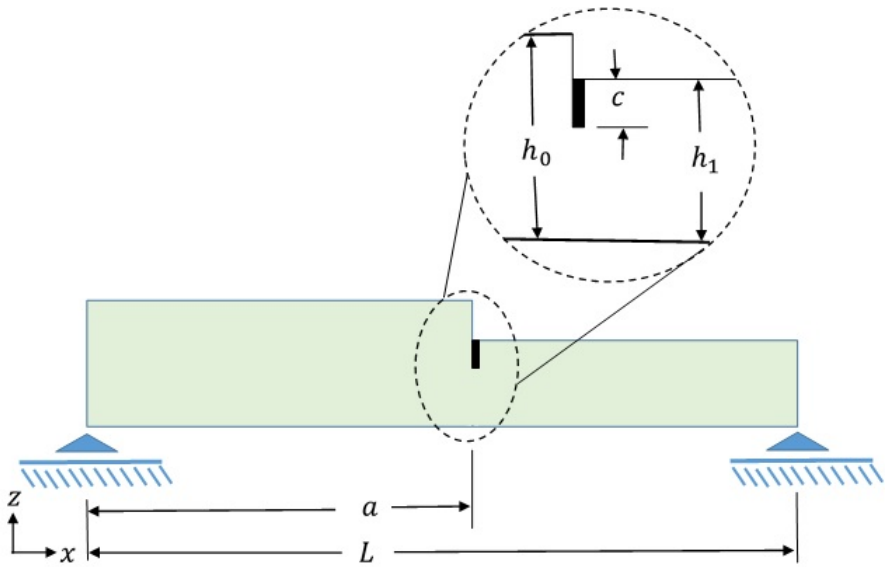

Figure 1. Geometry of the cracked and stepped nanobeam

the beam. So, there is a discontinuity at that location with different heights

$$h = \begin{cases} h_0, & x \in (0,a) \\ h_1, & x \in (a,L) \end{cases}. \tag{3.1}$$

The crack is treated as a stable crack whose depth is c (s is the ratio of crack depth and beam height).

3.2. Mathematical model

The equilibrium equation for the Euler–Bernoulli beam theory with rotatory inertia can be written as (see Reddy [65])

$$\frac{\partial^2 M}{\partial x^2} + N\frac{\partial^2 W}{\partial x^2} = I_0\frac{\partial^2 W}{\partial t^2} - I_r\frac{\partial^4 W}{\partial x^2 \partial t^2}, \tag{3.2}$$

in which I_0 presents the second moment of area and E is the modulus of elasticity. N denotes the axial force that is considered constant throughout the beam. I_r represents the rotatory inertia as $I_r = \rho\int_{-h/2}^{h/2} z^2 dA$, ρ is the density of the material and t is the time. Applying the nonlocal theory (2.7) and Euler-Bernoulli beam theory (3.2), the governing equation for nanobeams can be written as

$$\begin{aligned} EI\frac{\partial^4 W}{\partial x^4} - (e_0 a)^2\left(-N\frac{\partial^4 W}{\partial x^4} + I_0\frac{\partial^4 W}{\partial x^2\partial t^2} - I_r\frac{\partial^6 W}{\partial x^4\partial t^2}\right) \\ -N\frac{\partial^2 W}{\partial x^2} + I_0\frac{\partial^2 W}{\partial t^2} - I_r\frac{\partial^4 W}{\partial x^2\partial t^2} = 0. \end{aligned} \tag{3.3}$$

Using the transformation (2.11) and non-dimensional parameters (2.12), the equation (3.3) can be simplified as follows

$$\left(1+\mu^2 n - \mu^2 r_0\omega_0^2\right)\frac{d^4 w}{d\xi^4} + \left(\mu^2\omega_0^2 - n + r_0\omega_0^2\right)\frac{d^2 w}{d\xi^2} - \omega_0^2 w = 0, \tag{3.4}$$

where

$$I_0 = \rho,\ \ r_0 = \frac{1}{12}\left(\frac{h_0}{L}\right)^2,\ \ \gamma = \frac{h_1}{h_0},\ \ \omega_1 = \gamma\omega_0.$$

Here, r_0 indicate the effect of rotatory inertia, γ is the step heights ratio, h_0, h_1 are the height of the two segments, respectively. ω_0, ω_1 are the dimensionless frequency for two different segments of the beam. Considering the two segments of the beam, the equation (3.4) can be written as follows

$$\frac{d^4 w}{d\xi^4} + \frac{\beta_0}{\alpha_0}\frac{d^2 w}{d\xi^2} - \frac{\omega_0^2}{\alpha_0}w = 0,\ \text{ for }\ \xi \in (0,a), \tag{3.5}$$

and

$$\frac{d^4 w}{d\xi^4} + \frac{\beta_1}{\alpha_1}\frac{d^2 w}{d\xi^2} - \frac{\omega_1^2}{\alpha_1}w = 0,\ \text{ for }\ \xi \in (a,1), \tag{3.6}$$

where

$$\alpha_0 = 1+\mu^2 n-\mu^2 r_0\omega_0^2, \qquad \beta_0 = \mu^2\omega_0^2 - n + r_0\omega_0^2,$$

and

$$\alpha_1 = 1+\mu^2 n-\mu^2 r_1\omega_1^2, \qquad \beta_1 = \mu^2\omega_1^2 - n + r_1\omega_1^2.$$

3.3. Solution

Using the basic principle of the homotopy perturbation method (HPM), we can write the governing equation for $x \in (0,a)$ as

$$(1-P)\left(\frac{d^4w}{d\xi^4} - \frac{d^4w_0}{d\xi^4}\right) + P\left(\frac{d^4w}{d\xi^4} + \frac{\beta_0}{\alpha_0}\frac{d^2w}{d\xi^2} - \frac{\omega_0^2}{\alpha_0}w\right) = 0, \tag{3.7}$$

for $x \in (a,L)$ as

$$(1-P)\left(\frac{d^4w}{d\xi^4} - \frac{d^4w_0}{d\xi^4}\right) + P\left(\frac{d^4w}{d\xi^4} + \frac{\beta_1}{\alpha_1}\frac{d^2w}{d\xi^2} - \frac{\omega_1^2}{\alpha_1}w\right) = 0, \tag{3.8}$$

here, P is the perturbation constant. We consider the initial approximations (w_0) for two different segments as follows

$$w_0 = A_0 + \xi A_1 + \frac{1}{2}\xi^2 A_2 + \frac{1}{6}\xi^3 A_3, \quad x \in (0,a) \tag{3.9}$$

and

$$w_0 = A_4 + \xi A_5 + \frac{1}{2}\xi^2 A_6 + \frac{1}{6}\xi^3 A_7, \quad x \in (a,1), \tag{3.10}$$

here, $A_0, ..., A_7$ are constants. Using the initial approximation, one can calculate the other terms $(w_1, w_2, w_3, ..., w_n)$ of the governing equations. Using the boundary and intermediate conditions, eight algebraic equations are formed with eight unknowns. These equations can be presented in a matrix form as

$$\left[M(\omega_0)\right]\begin{bmatrix} A_0 \\ A_2 \\ A_3 \\ \dots \\ A_6 \\ A_7 \end{bmatrix} = 0. \tag{3.11}$$

Here, M is the coefficient matrix. Solving the determinant of the matrix, one can find the nontrivial solution. The real value of ω_0 represents the natural frequency of nanobeams. This problem is solved using the exact solution technique (see Hossain and Lellep [28-31], Motaghiana et al. [58]). The results of both techniques are compared favorably.

Table 1. The frequency of nanobeams for different values of the nonlocal parameter

		SS		CS		CC	
μ	Mode	HPM	Exact	HPM	Exact	HPM	Exact
0	1	9.981445	9.869384	15.51445	15.41723	22.51406	22.37353
0	2	39.80859	39.47705	50.22031	49.96533	61.95312	61.67138
0	3	90.64375	88.82519	107.1218	104.2412	125.6960	120.9042
0.5	1	5.406738	5.300292	7.942382	7.784423	11.21069	10.99121
0.5	2	12.21386	11.97485	14.98398	14.68701	24.80932	24.33398
0.5	3	18.803 71	18.43798	21.68398	21.25610	31.07802	30.48632

Table 2. The frequency of nanobeams for different values of length to height ratio

		SS		CS		CC	
L/h	Mode	HPM	Exact	HPM	Exact	HPM	Exact
100	1	9.607031	9.411523	14.88769	14.58496	21.50297	21.06894
100	2	33.81835	33.26757	42.24589	41.48828	51.34238	50.434 17
100	3	65.35546	63.53564	74.71484	73.15234	84.91113	83.19316
20	1	9.511230	9.321679	14.55371	14.27050	20.55322	20.17104
20	2	30.44335	30.03339	36.18554	35.70507	41.46464	40.974 80
20	3	47.87109	47.13593	51.24609	50.73046	54.23222	53.77070

3.4. Results and discussion

In this section, the dynamic behavior of stepped and cracked nanobeams is solved by the homotopy perturbation method (HPM) and the exact solution method. At first, the accuracy of the analysis is measured by comparing the results of HPM with the results of the exact solution technique. Then, the effect of nonlocal parameter, step and crack location, and crack depth on natural frequency are presented for different boundary conditions such as simply supported (SS), clamped simply (CS), and fully clamped (CC). The results of the calculation are described in Tables 1, 2 and Figures 2–5.

Table 1 presents the natural frequency for different support systems. Different modes of frequency and different values of the nonlocal parameter are also considered. It is clear from this table that the natural frequency decreases rapidly with the increase of the nonlocal parameter. Table 2 illustrates the effect of rotatory inertia on the natural frequency of nanobeams under different support systems. It is clearly described that natural frequency decreases with the decrease of the length to height ratio. Thus the effect of rotatory inertia can be ignored in a slender beam.

Figures 2, and 3 describe the effect of crack depth on the natural frequency of nanobeams for different modes of frequency and different boundary conditions such as fully clamped (CC), and clamped simply (CS). It can be seen from these graphs that natural frequency decreases with the increase of crack depth. In the first mode, when the crack depth is more than 0.4 then rotatory inertia has no

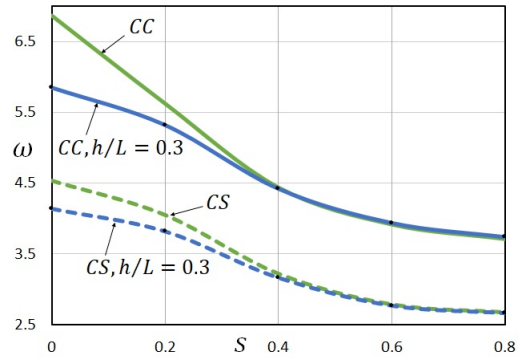

Figure 2. Frequency versus crack depth in first mode

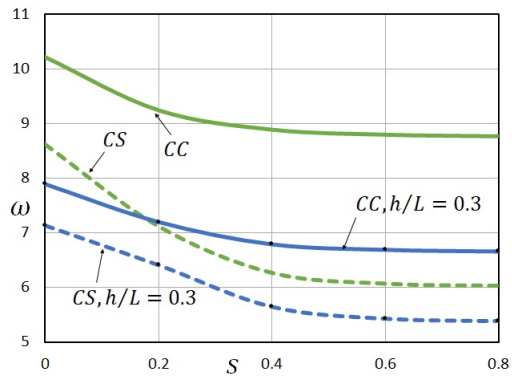

Figure 3. Frequency versus crack depth in second mode

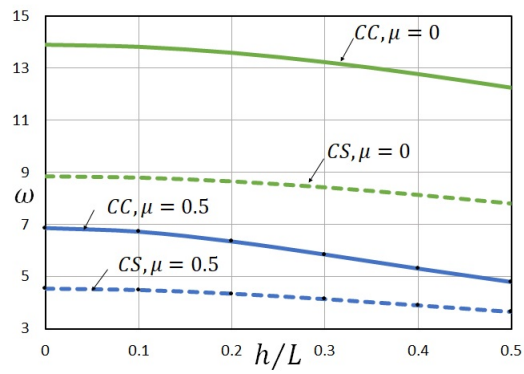

Figure 4. Frequency versus height to length ratio in first mode

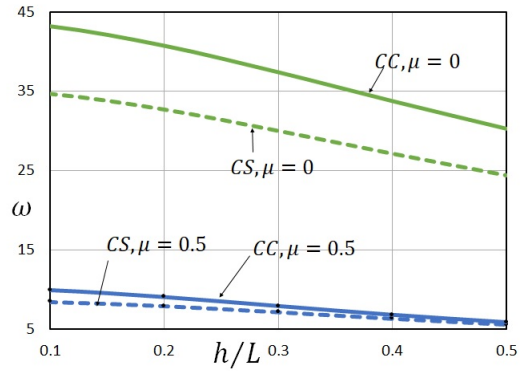

Figure 5. Frequency versus height to length ratio in second mode

effect. On the other hand, rotatory inertia is more significant in the second mode than in the first mode of frequency.

Figures 4, and 5 describe the effect of the height to length ratio on the natural frequency of nanobeams for different modes of frequency and different boundary conditions such as fully clamped (CC), and clamped simply (CS). It is clear from these graphs that natural frequency decreases with the increase of the height to length ratio. In the second mode of frequency, the natural frequency decreases more rapidly than in the first mode of frequency.

4. FREE VIBRATION ANALYSIS OF THE TAPERED CRACKED DOUBLE NANOBEAMS USING MACLAURIN SERIES

In this section, the Maclaurin series technique is applied to analyze the vibration of the cracked tapered double nanobeams according to the paper by Hossain and Lellep [35].

4.1. Physical description

A schematic shape of a double nanobeam (see Li et al. [50]) consists of two parallel nanobeams connected to each other by distributed vertical Winkler-type springs. The two nanobeams are referred to as the upper beam and the lower beam. Nanobeams are assumed to be slender and satisfy the Euler-Bernoulli beam theory. The origin of the coordinate system (x, y, z) is considered to be at the left endpoint of the beam. Both nanobeams are assumed to be made of the same material. Therefore, physical and geometrical properties are considered to be the same for both beams. A crack is considered as a defect on the upper beam.

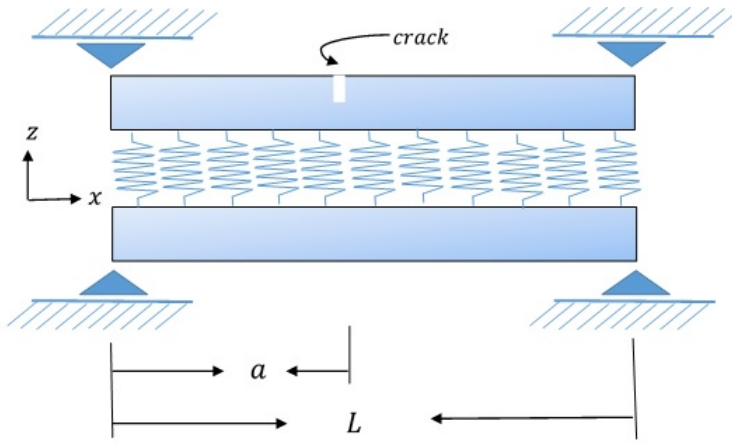

Figure 6. A cracked tapered double nanobeam

4.1.1. Governing equations

A double beam consists of two beams with identical material and geometric properties. Combining the classical beam theory (2.10) and the nonlocal theory of

elasticity (2.7), coupled equations for the double nanobeam can be written as

$$\begin{aligned}
&\frac{\partial^2}{\partial x^2}\left(EI(x)\frac{\partial^2 W_1}{\partial x^2}\right)+\rho A(x)\frac{\partial^2 W_1}{\partial t^2}-(e_0a_0)^2\frac{\partial^2}{\partial x^2}\left(\rho A(x)\frac{\partial^2 W_1}{\partial t^2}\right)\\
&\qquad +K_s\frac{b(x)}{b_0}(W_1-W_2)-(e_0a_0)^2K_s\frac{\partial^2}{\partial x^2}\frac{b(x)}{b_0}(W_1-W_2)=0,\\
&\frac{\partial^2}{\partial x^2}\left(EI(x)\frac{\partial^2 W_2}{\partial x^2}\right)+\rho A(x)\frac{\partial^2 W_2}{\partial t^2}-(e_0a_0)^2\frac{\partial^2}{\partial x^2}\left(\rho A(x)\frac{\partial^2 W_2}{\partial t^2}\right)\\
&\qquad +K_s\frac{b(x)}{b_0}(W_2-W_1)-(e_0a_0)^2K_s\frac{\partial^2}{\partial x^2}\frac{b(x)}{b_0}(W_2-W_1)=0,
\end{aligned}\tag{4.1}$$

where W_1 and W_2 are the deflection of upper and lower beams in the double nanobeam, respectively. K_s is the spring constant. Both beams in the double beam are tapered along the x-axis. Applying geometric properties of the tapered beam (2.32), the equation (4.1) can be expressed as

$$\begin{aligned}
&\frac{\partial^2}{\partial x^2}\left(EI_0e^{\frac{\alpha x}{L}}\frac{\partial^2 W_1}{\partial x^2}\right)+\rho A_0e^{\frac{\alpha x}{L}}\frac{\partial^2 W_1}{\partial t^2}-(e_0a_0)^2\frac{\partial^2}{\partial x^2}\left(\rho A_0e^{\frac{\alpha x}{L}}\frac{\partial^2 W_1}{\partial t^2}\right)\\
&\qquad +K_s\frac{b_0}{b_0}e^{\frac{\alpha x}{L}}(W_1-W_2)-(e_0a_0)^2K_s\frac{\partial^2}{\partial x^2}\frac{b_0}{b_0}e^{\frac{\alpha x}{L}}(W_1-W_2)=0,\\
&\frac{\partial^2}{\partial x^2}\left(EI_0e^{\frac{\alpha x}{L}}\frac{\partial^2 W_2}{\partial x^2}\right)+\rho A_0e^{\frac{\alpha x}{L}}\frac{\partial^2 W_2}{\partial t^2}-(e_0a_0)^2\frac{\partial^2}{\partial x^2}\left(\rho A_0e^{\frac{\alpha x}{L}}\frac{\partial^2 W_2}{\partial t^2}\right)\\
&\qquad +K_s\frac{b_0}{b_0}e^{\frac{\alpha x}{L}}(W_2-W_1)-(e_0a_0)^2K_s\frac{\partial^2}{\partial x^2}\frac{b_0}{b_0}e^{\frac{\alpha x}{L}}(W_2-W_1)=0,
\end{aligned}\tag{4.2}$$

where α is the tapered ratio. These partial differential equations can be transformed into ordinary differential equations using the transformation (2.11) and dimensionless parameters (2.12). Therefore, the equation (4.2) can be presented as

$$\begin{aligned}
&\frac{d^4w_1}{d\xi^4}+2\alpha\frac{d^3w_1}{d\xi^3}+(\mu^2\omega^2-k_s\mu^2+\alpha^2)\frac{d^2w_1}{d\xi^2}+(2\alpha\mu^2\omega^2-2\alpha k_s\mu^2)\frac{dw_1}{dx}\\
&\qquad +(\alpha^2\mu^2\omega^2-\alpha^2k_s\mu^2-\omega^2+k_s)w_1+\mu^2k_s\frac{d^2w_2}{dx^2}\\
&\qquad +2\mu^2k_s\alpha\frac{dw_2}{dx}+(\alpha^2k_s\mu^2-k_s)w_2=0,\\
&\frac{d^4w_2}{d\xi^4}+2\alpha\frac{d^3w_2}{d\xi^3}+(\mu^2\omega^2-k_s\mu^2+\alpha^2)\frac{d^2w_2}{d\xi^2}+(2\alpha\mu^2\omega^2-2\alpha k_s\mu^2)\frac{dw_2}{dx}\\
&\qquad +(\alpha^2\mu^2\omega^2-\alpha^2k_s\mu^2-\omega^2+k_s)w_2+\mu^2k_s\frac{d^2w_1}{dx^2}\\
&\qquad +2\mu^2k_s\alpha\frac{dw_1}{dx}+(\alpha^2k_s\mu^2-k_s)w_1=0,
\end{aligned}\tag{4.3}$$

here, w_1, w_2 are the dimensionless deflection of upper and lower beams, $k_s=\frac{K_sL^4}{EI}$ is the dimensionless spring constant. These equations (4.3) are the governing

equations of the double nanobeam in simplified form. These equations can be solved numerically.

4.2. Solution technique

Deformations of a double nanobeam are presented by coupled differential equations (4.3). These governing equations can be presented as follows

$$\begin{aligned}
\frac{d^4w_1}{d\xi^4} &= -2\alpha\frac{d^3w_1}{d\xi^3} - (\mu^2\omega^2 - k_s\mu^2 + \alpha^2)\frac{d^2w_1}{d\xi^2} \\
&-(2\alpha\mu^2\omega^2 - 2\alpha k_s\mu^2)\frac{dw_1}{d\xi} - (\alpha^2\mu^2\omega^2 - \alpha^2 k_s\mu^2 \\
&-\omega^2 + k_s)w_1 - \mu^2 k_s\frac{d^2w_2}{d\xi^2} - 2\mu^2 k_s\alpha\frac{dw_2}{d\xi} - (\alpha^2 k_s\mu^2 - k_s)w_2, \\
\frac{d^4w_2}{d\xi^4} &= -2\alpha\frac{d^3w_2}{d\xi^3} - (\mu^2\omega^2 - k_s\mu^2 + \alpha^2)\frac{d^2w_2}{d\xi^2} \\
&-(2\alpha\mu^2\omega^2 - 2\alpha k_s\mu^2)\frac{dw_2}{d\xi} - (\alpha^2\mu^2\omega^2 - \alpha^2 k_s\mu^2 \\
&-\omega^2 + k_s)w_2 - \mu^2 k_s\frac{d^2w_1}{d\xi^2} - 2\mu^2 k_s\alpha\frac{dw_1}{d\xi} - (\alpha^2 k_s\mu^2 - k_s)w_1.
\end{aligned} \tag{4.4}$$

Differentiating the equations (4.4), one can express as

$$\begin{aligned}
\frac{d^5w_1}{d\xi^5} &= -2\alpha\frac{d^4w_1}{d\xi^4} - (\mu^2\omega^2 - k_s\mu^2 + \alpha^2)\frac{d^3w_1}{d\xi^3} \\
&-(2\alpha\mu^2\omega^2 - 2\alpha k_s\mu^2)\frac{d^2w_1}{d\xi^2} - (\alpha^2\mu^2\omega^2 - \alpha^2 k_s\mu^2 - \omega^2 + k_s)\frac{w_1}{d\xi} \\
&-\mu^2 k_s\frac{d^3w_2}{d\xi^3} - 2\mu^2 k_s\alpha\frac{d^2w_2}{d\xi^2} - (\alpha^2 k_s\mu^2 - k_s)\frac{dw_2}{d\xi}, \\
\frac{d^5w_2}{d\xi^5} &= -2\alpha\frac{d^4w_2}{d\xi^4} - (\mu^2\omega^2 - k_s\mu^2 + \alpha^2)\frac{d^3w_2}{d\xi^3} \\
&-(2\alpha\mu^2\omega^2 - 2\alpha k_s\mu^2)\frac{d^2w_2}{d\xi^2} - (\alpha^2\mu^2\omega^2 - \alpha^2 k_s\mu^2 - \omega^2 + k_s)\frac{w_2}{d\xi} \\
&-\mu^2 k_s\frac{d^3w_1}{d\xi^3} - 2\mu^2 k_s\alpha\frac{d^2w_1}{d\xi^2} - (\alpha^2 k_s\mu^2 - k_s)\frac{dw_1}{d\xi}.
\end{aligned} \tag{4.5}$$

Substituting $\frac{d^4w_1}{d\xi^4}$ and $\frac{d^4w_2}{d\xi^4}$ in the equations (4.5), one can express as

$$\begin{aligned}
\frac{d^5w_1}{d\xi^5} &= (-\mu^2\omega^2 + k_s\mu^2 + 3\alpha^2)\frac{d^3w_1}{d\xi^3} + 2\alpha^3\frac{d^2w_1}{d\xi^2} \\
&+(3\alpha^2\mu^2\omega^2 - 3\alpha^2k_s\mu^2 + \omega^2 - k_s)\frac{dw_1}{d\xi} - 2\alpha(-\alpha^2\mu^2\omega^2 + \alpha^2k_s\mu^2 \\
&+\omega^2 - k_s)w_1 - k_s\mu^2\frac{d^3w_2}{d\xi^3} + (3\alpha^2k_s\mu^2 + k_s)\frac{dw_2}{d\xi} + 2\alpha k_s(\alpha^2\mu^2 - 1)w_2, \\
\frac{d^5w_2}{d\xi^5} &= (-\mu^2\omega^2 + k_s\mu^2 + 3\alpha^2)\frac{d^3w_2}{d\xi^3} + 2\alpha^3\frac{d^2w_2}{d\xi^2} \\
&+(3\alpha^2\mu^2\omega^2 - 3\alpha^2k_s\mu^2 + \omega^2 - k_s)\frac{dw_2}{d\xi} - 2\alpha(-\alpha^2\mu^2\omega^2 + \alpha^2k_s\mu^2 \\
&+\omega^2 - k_s)w_2 - k_s\mu^2\frac{d^3w_1}{d\xi^3} + (3\alpha^2k_s\mu^2 + k_s)\frac{dw_1}{d\xi} + 2\alpha k_s(\alpha^2\mu^2 - 1)w_1.
\end{aligned} \tag{4.6}$$

Similarly, one can calculate $\frac{d^6w_1}{d\xi^6}$, $\frac{d^6w_2}{d\xi^6}$, $\frac{d^7w_1}{d\xi^7}$, $\frac{d^7w_2}{d\xi^7}$, ..., upto n^{th} order derivative. Let us consider the values of derivatives at zero as follows

$$\begin{aligned}
w_1(0) = c_0, \quad w_2(0) = d_0, \\
\frac{dw_1}{d\xi}(0) = c_1, \quad \frac{dw_2}{d\xi}(0) = d_1, \\
\frac{d^2w_1}{d\xi^2}(0) = c_2, \quad \frac{d^2w_2}{d\xi^2}(0) = d_2, \\
\frac{d^3w_1}{d\xi^3}(0) = c_3, \quad \frac{d^3w_2}{d\xi^3}(0) = d_3.
\end{aligned} \tag{4.7}$$

Using the equations (4.7), higher derivatives at zero can be expressed as

$$\begin{aligned}
\frac{d^4w_1}{d\xi^4}(0) &= (-\alpha^2\mu^2\omega^2+\alpha^2k_s\mu^2+\omega^2-k_s)c_0\\
&+(-2\alpha\mu^2\omega^2+2\alpha k_s\mu^2)c_1+(-\mu^2\omega^2+k_s\mu^2-\alpha^2)c_2+(-2\alpha)c_3\\
&+(-\alpha^2k_s\mu^2+k_s)d_0+(-2\alpha k_s\mu^2)d_1+(-k_s\mu^2)d_2,\\
\frac{d^4w_2}{d\xi^4}(0) &= (-\alpha^2\mu^2\omega^2+\alpha^2k_s\mu^2+\omega^2-k_s)d_0\\
&+(-2\alpha\mu^2\omega^2+2\alpha k_s\mu^2)d_1+(-\mu^2\omega^2+k_s\mu^2-\alpha^2)d_2+(-2\alpha)d_3\\
&+(-\alpha^2k_s\mu^2+k_s)c_0+(-2\alpha k_s\mu^2)c_1+(-k_s\mu^2)c_2,\\
\frac{d^5w_1}{d\xi^5}(0) &= (2\alpha^3\mu^2\omega^2-2\alpha^3k_s\mu^2-2\alpha\omega^2+2\alpha k_s)c_0+(3\alpha^2\mu^2\omega^2\\
&-3\alpha^2k_s\mu^2+\omega^2-k_s)c_1+2\alpha^3c_2+(-\mu^2\omega^2+k_s\mu^2+3\alpha^2)c_3\\
&+(2\alpha^3k_s\mu^2-2\alpha k_s)d_0+(3\alpha^2k_s\mu^2+k_s)d_1-k_s\mu^2d_3,\\
\frac{d^5w_2}{d\xi^5}(0) &= (2\alpha^3\mu^2\omega^2-2\alpha^3k_s\mu^2-2\alpha\omega^2+2\alpha k_s)d_0+(3\alpha^2\mu^2\omega^2\\
&-3\alpha^2k_s\mu^2+\omega^2-k_s)d_1+2\alpha^3d_2+(-\mu^2\omega^2+k_s\mu^2+3\alpha^2)d_3\\
&+(2\alpha^3k_s\mu^2-2\alpha k_s)c_0+(3\alpha^2k_s\mu^2+k_s)c_1-k_s\mu^2c_3.
\end{aligned} \tag{4.8}$$

Using the equations (4.7, 4.8), one can present an approximate solution according to the Maclaurin series as follows

$$\begin{aligned}
w_1(\xi) &= c_0+c_1\xi+\frac{1}{2}c_2\xi^2+\frac{1}{6}c_3\xi^3\\
&+\frac{1}{24}(-\alpha^2\mu^2\omega^2c_0+\alpha^2k_s\mu^2c_0-\alpha^2k_s\mu^2d_0+...)\xi^4\\
&+\frac{1}{120}(2\alpha^3\mu^2\omega^2c_0-2\alpha^3k_s\mu^2c_0+2\alpha^3k_s\mu^2d_0+...)\xi^5+...,\\
w_2(\xi) &= d_0+d_1\xi+\frac{1}{2}d_2\xi^2+\frac{1}{6}d_3\xi^3\\
&+\frac{1}{24}(-\alpha^2\mu^2\omega^2d_0+\alpha^2k_s\mu^2d_0-\alpha^2k_s\mu^2c_0+...)\xi^4\\
&+\frac{1}{120}(2\alpha^3\mu^2\omega^2d_0-2\alpha^3k_s\mu^2d_0+2\alpha^3k_s\mu^2c_0+...)\xi^5+... \quad .
\end{aligned} \tag{4.9}$$

The equations (4.9) include eight constants $(c_0,...,c_3,d_0,...,d_3)$. In order to eliminate these constants and find the natural frequency, one can use the boundary conditions (2.13-2.16). Let us consider boundary conditions for the simply supported double nanobeam. Now, the equations (4.9) can be transformed into matrix form as follows

$$\begin{bmatrix} 1 & ... & 0 \\ ... & ... & ... \\ \frac{1}{2}k_s-\frac{1}{3}ak_s+... & ... & 1+\frac{1}{6}k_s\mu^2-... \end{bmatrix}\begin{bmatrix} c_0 \\ ... \\ d_3 \end{bmatrix}=0. \tag{4.10}$$

Solving the equation (4.10), one can find the natural frequency of the double nanobeam.

4.2.1. Cracked double nanobeams

A crack divides the double nanobeam into two double nanobeams. Therefore, the crack divides the double nanobeam into four segments. Four series solutions are needed to study the cracked double nanobeam. There are sixteen constants in the four series. Additional conditions are

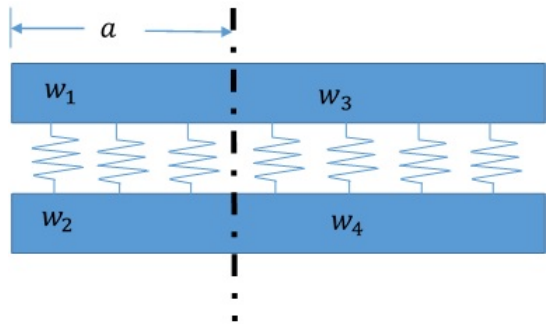

Figure 7. Modeling of the crack

for upper layer

$$w'_1 + K_1 w''_1 - w'_3 = 0, \tag{4.11}$$

and for lower layer

$$w'_2 + K_2 w''_2 - w'_4 = 0. \tag{4.12}$$

If a single crack is at the upper beam then crack severity is needed to consider K for the upper beam and the lower beam crack severity will be zero. A similar condition is applicable when the crack is only at the lower beam. When cracks are at both upper and lower beams then crack severities K_1, K_2 are needed to consider for the upper and lower beams, respectively.

4.3. Results and discussion

In this section, numerical analysis is performed to express the effects of some parameters on the dynamic behavior of cracked tapered double nanobeam systems using tables and graphs. Here, different boundary conditions such as simply supported (SS), fully clamped (CC), clamped simply (CS), and clamped free (CF) are considered.

4.3.1. Validation and verification

In this section, obtained results are verified by comparing the results with the results of other researchers in the literature. Table 3 describes the natural frequency

of the simply supported double nanobeam where beams are considered as identical beams having rectangular cross-sections. It is seen from this table that the present results are closely matched with the results of the reference paper (Sari et al. [69]).

Table 3. Verification of frequency for various values of the spring constant and nonlocal parameter

k_s	μ	References	ω_1	ω_2	ω_3
100	0.2	Sari et al. [69]	8.3569	16.4267	24.5823
		Present	8.3569	16.4267	24.5839
	0.4	Sari et al. [69]	6.1456	14.5951	15.4197
		Present	6.1459	14.5947	15.4189
500	0.2	Sari et al. [69]	8.3569	24.5823	32.7084
		Present	8.3573	24.5839	32.7089
	0.4	Sari et al. [69]	6.1456	14.5951	22.7743
		Present	6.1469	14.5888	22.2324

Table 4. Frequency of the simply supported double nanobeam for various values of the taper ratio, nonlocal parameter and crack severity

α	μ	K	ω_1	ω_2	ω_3	ω_4	ω_5	ω_6
2	0	0	9.4868	22.1347	39.8554	44.5898	89.4140	91.6015
		0.3	8.7846	21.8222	35.5332	43.1601	85.6328	90.7578
	0.2	0	8.1079	21.5800	24.9785	31.9980	41.9726	46.2382
		0.3	7.4868	20.3457	22.8457	30.0605	40.2851	45.3164
0	0	0	9.8701	22.3027	39.4804	44.2539	88.8203	91.0546
		0.3	9.2837	22.0214	34.5019	42.7460	83.7734	90.1484
	0.2	0	8.3569	21.6738	24.5839	31.6894	41.6211	46.1757
		0.3	7.8217	20.0761	22.5332	29.7129	39.7929	45.1758

4.3.2. Effects of crack locations

The location of the crack is very significant as like as crack severity. In a simply supported beam crack at the support does not influence the natural frequency. Figures 8 and 9 describe the effect of crack location on the natural frequency for the simply supported nanobeam. In this section, nonlocal parameter, spring constant, and taper ratio are considered $\mu = 0.1$, $k_s = 200$, $\alpha = 0$, respectively. At some specific locations, an increase in crack severity decreases the natural frequency.

4.3.3. Mode shape analysis

Mode shape is a significant measure to predict the dynamic behavior of structural elements. Basically, the mode shape describes the transverse displacement from

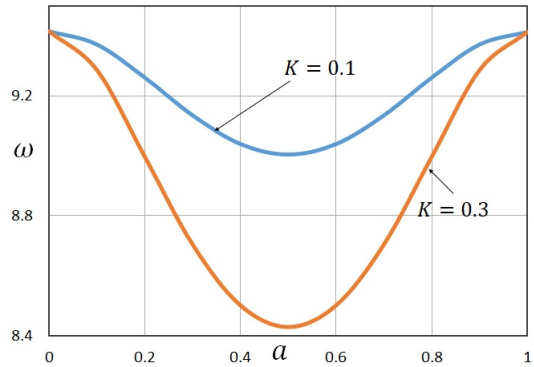

Figure 8. Frequency versus crack location with different values of crack severity (SS, first mode)

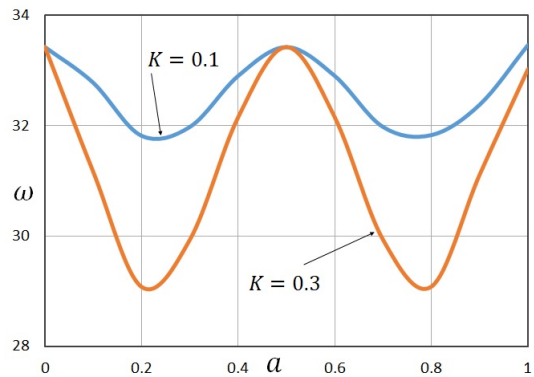

Figure 9. Frequency versus crack location with different values of crack severity (SS, second mode)

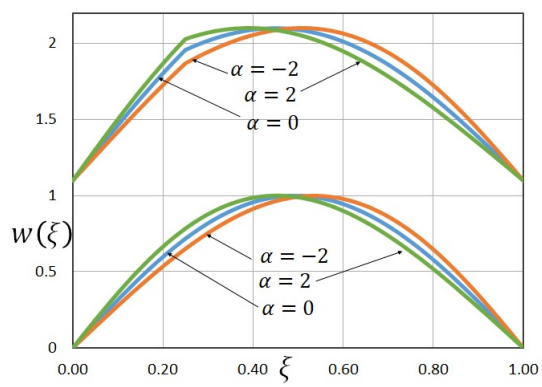

Figure 10. Mode shape of the double nanobeam for different values of taper ratio (first mode, SS)

Table 5. Frequency of the double tapered nanobeam for different values of taper ratio and boundary conditions

	$\alpha = 2$			$\alpha = 0$		
BC	ω_1	ω_2	ω_3	ω_1	ω_2	ω_3
SS SS	9.0767	16.8037	33.8652	9.4155	16.9893	33.4277
CC CC	21.7480	25.9433	51.7539	21.1074	25.4082	50.9805
CC SS	12.6416	24.3926	35.2363	12.7959	23.8808	34.8027
CF CF	1.9510	14.2764	17.7314	3.5315	14.5771	20.6777
CS CS	12.6611	18.9814	40.7461	14.5986	20.3262	41.7929

Table 6. Frequency of the simply supported double nanobeam for various values of the spring constant and crack severity

K	k_s	ω_1	ω_2	ω_3	ω_4	ω_5	ω_6
0	50	9.3306	13.6767	33.5371	34.9941	64.7695	65.5586
	250	9.3306	24.2285	33.5371	40.3086	64.7773	68.5273
	2000	9.3306	33.5371	63.9804	64.6914	71.6523	89.8672
0.3	50	8.6177	13.2471	28.4707	34.3574	60.8086	65.1914
	250	8.7075	23.7558	29.8223	38.5176	61.6679	67.3164
	2000	8.7827	30.5293	60.9258	63.9648	69.8008	87.9766

the neutral axis during vibration. Figures 10, and 11 illustrate the mode shapes for simply supported nanobeams with various values of taper ratio. A crack is considered only at the upper beam and the lower beam is fully intact. Crack severity $K = 0.3$, crack location $a = 0.25$, spring constant $k_s = 200$, nonlocal parameter $\mu = 0.1$ are considered, respectively. It is seen from these figures that mode shapes are influenced by the taper ratio. This influence increases at a higher mode of frequency. A crack at the upper beam affects the mode shape of the upper beam as well as the lower beam significantly.

4.3.4. Parametric effects

Parametric analysis is essential to comprehend the dynamic behavior of the double nanobeam properly. Natural frequency is influenced by the spring constant, nonlocal parameter, taper ratio, crack severity, and boundary conditions significantly. Table 4 describes the frequency of the simply supported double nanobeam for several values of the taper ratio, nonlocal parameter, and crack severity. A crack is considered at the location of $a = 0.25$ and spring constant $k_s = 200$ is considered. In a simply supported beam, frequency is higher in the rectangular beam than in the tapered beam. Table 5 illustrates the frequency of the double tapered nanobeam for different boundary conditions and taper ratios. The beam is considered intact where $K = 0$ and $\mu = 0.1$. In clamped beam, frequency is higher in the tapered beam than in the rectangular beam. Table 6 represents the

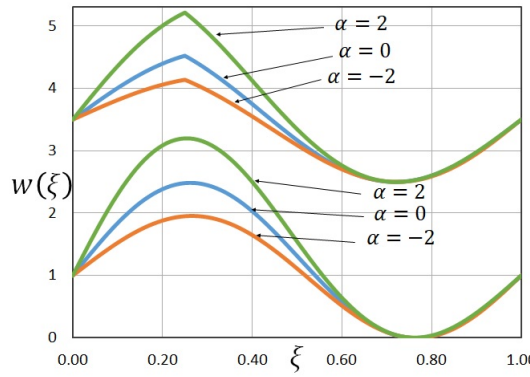

Figure 11. Mode shape of the double nanobeam for different values of taper ratio (second mode, SS)

frequency of the simply supported double nanobeam for various spring constants and crack severities where $\alpha = 1$, $\mu = 0.1$, and $a = 0.25$ are considered. Frequency increases for the increase of the spring constant. Whereas, the first mode of frequency is less effective than the higher mode of frequency for the increase of the spring constant.

5. TRANSVERSE VIBRATION OF TAPERED NANOBEAMS WITH ELASTIC SUPPORTS

A solution technique based on the homotopy perturbation method is proposed to analyze the dynamic behavior of the tapered nanobeam with elastic supports (see Hossain and Lellep [32]).

5.1. Problem description

A schematic shape of a linearly elastic, isotropic, tapered nanobeam subjected to transverse vibration is illustrated in Figure 12.

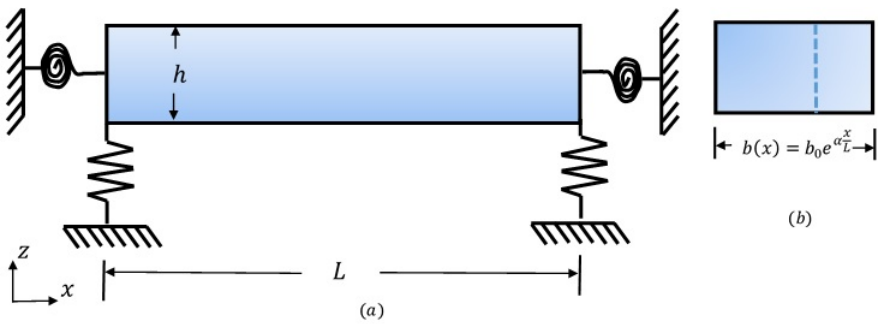

Figure 12. (a) A tapered nanobeam with elastic supports, (b) Tapered cross-section

Let the origin of the coordinate system be placed at the left end of the nanobeam. The beam axis coincides with the x-axis and the height of the beam is parallel to the z-axis. The nanobeam with length L and variable-width $b(x)$ are considered. The modulus of elasticity E and the density of the beam ρ are uniform throughout the beam. Translational and rotational flexible supports are used at both ends of the beam. Our intention is to find the effects of the taper ratio and the nonlocal parameter on the natural vibration of nanobeams.

5.2. Mathematical model

Combining the equations (2.7), and (2.10) and eliminating axial force N, the bending moment M for the nonlocal beam model can be expressed as

$$M = -(e_0 a)^2 (-\rho A(x) \frac{\partial^2 W}{\partial t^2}) - EI(x) \frac{\partial^2 W}{\partial x^2}. \tag{5.1}$$

Similarly, from the equation (5.1), the shear force Q for the nonlocal beam model can be presented as

$$Q = -(e_0 a)^2 \frac{\partial}{\partial x} (-\rho A(x) \frac{\partial^2 W}{\partial t^2}) - \frac{\partial}{\partial x} (EI(x) \frac{\partial^2 W}{\partial x^2}). \tag{5.2}$$

Combining equations (5.1), and (2.10), the governing equation of the nonlocal tapered beam can be presented as

$$\frac{\partial^2}{\partial x^2}(EI(x)\frac{\partial^2 W}{\partial x^2})+(e_0a)^2\frac{\partial^2}{\partial x^2}(-\rho A(x)\frac{\partial^2 W}{\partial t^2})+\rho A(x)\frac{\partial^2 W}{\partial t^2}=0. \tag{5.3}$$

Substituting the values of $I(x)$ and $A(x)$ from equations (2.32), one can present (5.3) as

$$EI_0\frac{\partial^2}{\partial x^2}(e^{\frac{\alpha x}{L}}\frac{\partial^2 W}{\partial x^2})-(e_0a)^2\rho A_0\frac{\partial^2}{\partial x^2}(e^{\frac{\alpha x}{L}}\frac{\partial^2 W}{\partial t^2})+\rho A_0 e^{\frac{\alpha x}{L}}\frac{\partial^2 W}{\partial t^2}=0. \tag{5.4}$$

Applying the dimensionless parameters (2.12) and transformation function (2.11), equation (5.4) can be written as

$$\frac{d^2}{d\xi^2}(e^{\alpha\xi}\frac{d^2 w}{d\xi^2})+\mu^2\omega^2\frac{d^2}{d\xi^2}(e^{\alpha\xi}w)-\omega^2 e^{\alpha\xi}w=0. \tag{5.5}$$

Simplifying the equation (5.5), one can rewrite it as follows

$$\frac{d^4w}{d\xi^4}+2\alpha\frac{d^3w}{d\xi^3}+(\alpha^2+\mu^2\omega^2)\frac{d^2w}{d\xi^2}+2\alpha\mu^2\omega^2\frac{dw}{d\xi}+(\mu^2\omega^2\alpha^2-\omega^2)w=0. \tag{5.6}$$

Equation (5.6) is the simplified form of the governing equation. It is difficult to find the exact solution of this equation. However, it can be solved by the approximation technique.

5.2.1. Elastic boundary conditions

Elastic boundaries are modeled with the help of the flexible springs. In this paper, two types of spring boundary conditions are used. These are the rotational spring and translational spring. Rotational spring resists the moment at the boundary. On the other hand, translational spring resists shear at the boundary. The boundary conditions for the flexible supports are

$$T_0W=Q,\ \ R_0\frac{\partial W}{\partial x}=-M,\ \ at\quad x=0, \tag{5.7}$$

and

$$T_LW=-Q,\ \ R_L\frac{\partial W}{\partial x}=M,\ \ at\quad x=L, \tag{5.8}$$

where T_0, T_L represent spring constants for translational spring and R_0, R_L represent spring constants for rotational spring at the point $x=0$ and $x=L$, respectively. For the translational spring, from equations (5.7), and (5.2), it can be written as

$$T_0W=(e_0a)^2\frac{\partial}{\partial x}(\rho A(x)\frac{\partial^2 W}{\partial t^2})-\frac{\partial}{\partial x}(EI(x)\frac{\partial^2 W}{\partial x^2}). \tag{5.9}$$

Using the transformation (2.11) and dimensionless variable (2.12), the equation (5.9) can be written as

$$\frac{T_0L^3}{EI_0}w = -\mu^2\omega^2 e^{\alpha\xi}(\frac{\partial w}{\partial \xi}+\alpha w) - e^{\alpha\xi}(\frac{\partial^3 w}{\partial \xi^3}+\alpha\frac{\partial^2 w}{\partial \xi^2}). \tag{5.10}$$

The equation (5.10) can be presented as follows

$$t_0 w = -\mu^2\omega^2 e^{\alpha\xi}(\frac{\partial w}{\partial \xi}+\alpha w) - e^{\alpha\xi}(\frac{\partial^3 w}{\partial \xi^3}+\alpha\frac{\partial^2 w}{\partial \xi^2}). \tag{5.11}$$

where $t_0 = \frac{T_0L^3}{EI_0}$ is the dimensionless translational spring constant. If the origin of coordinates is the left boundary of the beam, the boundary condition can be written as follows

$$t_0 w = -\mu^2\omega^2(\frac{\partial w}{\partial \xi}+\alpha w) - (\frac{\partial^3 w}{\partial \xi^3}+\alpha\frac{\partial^2 w}{\partial \xi^2}). \tag{5.12}$$

Similarly for the rotational spring, according to the equations (5.7), and (5.1), it can be written as

$$R_0\frac{\partial W}{\partial x} = -(e_0a)^2\rho A(x)\frac{\partial^2 W}{\partial t^2} + EI(x)\frac{\partial^2 W}{\partial x^2}. \tag{5.13}$$

Using the transformation (2.11) and dimensionless variable (2.12), the equation (5.13) can be simplified as

$$r_0\frac{\partial w}{\partial \xi} = e^{\alpha\xi}\mu^2\omega^2 w + e^{\alpha\xi}\frac{\partial^2 w}{\partial \xi^2}. \tag{5.14}$$

where $r_0 = \frac{R_0L}{EI_0}$ is the dimensionless rotational spring constant. At the left corner of the beam, where $\xi = 0$, the equation (5.14) can be written as

$$r_0\frac{\partial w}{\partial \xi} = \mu^2\omega^2 w + \frac{\partial^2 w}{\partial \xi^2}. \tag{5.15}$$

In a similar way, from the equation (5.15), one can find the other two boundary conditions at $\xi = 1$ for translational and rotational springs as follows

$$t_L w = \mu^2\omega^2 e^{\alpha}(\alpha w + \frac{\partial w}{\partial \xi}) + e^{\alpha}(\alpha\frac{\partial^2 w}{\partial \xi^2}+\frac{\partial^3 w}{\partial \xi^3}), \tag{5.16}$$

and

$$r_L\frac{\partial w}{\partial \xi} = -\mu^2\omega^2 e^{\alpha} w + e^{\alpha}\frac{\partial^2 w}{\partial \xi^2}. \tag{5.17}$$

The required four boundary conditions for the connected springs at both ends of the beam can be presented as
at $\xi = 0$,

$$\begin{aligned} t_0 w + \mu^2\omega^2(\frac{\partial w}{\partial \xi} + \alpha w) + (\frac{\partial^3 w}{\partial \xi^3} + \alpha\frac{\partial^2 w}{\partial \xi^2}) = 0, \\ r_0\frac{\partial w}{\partial \xi} - \mu^2\omega^2 w - \frac{\partial^2 w}{\partial \xi^2} = 0, \end{aligned} \tag{5.18}$$

and at $\xi = 1$,

$$\begin{aligned} t_L w - \mu^2\omega^2 e^{\alpha}(\alpha w + \frac{\partial w}{\partial \xi}) - e^{\alpha}(\alpha\frac{\partial^2 w}{\partial \xi^2} + \frac{\partial^3 w}{\partial \xi^3}) = 0, \\ r_L\frac{\partial w}{\partial \xi} + \mu^2\omega^2 e^{\alpha} w + e^{\alpha}\frac{\partial^2 w}{\partial \xi^2} = 0. \end{aligned} \tag{5.19}$$

5.3. Solution of the problem

This problem can be solved using the homotopy perturbation method. Applying the basic rules of the homotopy perturbation method (2.39), the governing equation (5.6) of the problem can be written as

$$\begin{aligned} \frac{d^4 w}{d\xi^4} + P[2\alpha\frac{d^3 w}{d\xi^3} + (\alpha^2 + \mu^2\omega^2)\frac{d^2 w}{d\xi^2} \\ +2\alpha\mu^2\omega^2\frac{dw}{d\xi} + \omega^2(\mu^2\alpha^2 - 1)w] = 0. \end{aligned} \tag{5.20}$$

Considering the solution (2.40) of the equation (5.20), the coefficient of the power of P can be written as

$$\begin{aligned} P^0 \to \frac{d^4}{d\xi^4} w_0(\xi) = 0, \\ P^1 \to \frac{d^4}{d\xi^4} w_1(\xi) + 2\alpha(\frac{d^3}{d\xi^3} w_0(\xi)) + (\xi^2 + \mu^2\omega^2)(\frac{d^2}{d\xi^2} w_0(\xi)) \\ +2\alpha\mu^2\omega^2(\frac{d}{d\xi} w_0(\xi)) + (\mu^2\omega^2\alpha^2 - \omega^2) w_0 = 0, \\ P^2 \to \frac{d^4}{d\xi^4} w_2(\xi) + 2\alpha(\frac{d^3}{d\xi^3} w_1(\xi)) + (\alpha^2 + \mu^2\omega^2)(\frac{d^2}{d\xi^2} w_1(\xi) \\ +2\alpha\mu^2\omega^2(\frac{d}{d\xi} w_1(\xi)) + (\mu^2\omega^2\alpha^2 - \omega^2) w_1 = 0. \end{aligned} \tag{5.21}$$

The solution of the equation (5.21) is presented as follows

$$w_0 = A_0 + A_1\xi + A_2\frac{\xi^2}{2} + A_3\frac{\xi^3}{6}. \tag{5.22}$$

The remaining terms of the series can be calculated as

$$w_i = -2\alpha L^{-1}(\frac{d^3}{d\xi^3}w_{i-1}) - (\alpha^2+\mu^2\omega^2)L^{-1}(\frac{d^2}{d\xi^2}w_{i-1}) - \\ 2\alpha\mu^2\omega^2 L^{-1}(\frac{d}{d\xi}w_{i-1}) - (\mu^2\omega^2\alpha^2-\omega^2)L^{-1}(w_{i-1}), \tag{5.23}$$

where $i = 1,2,3,...,n$ and $L^{-1} = \int\int\int\int d\xi d\xi d\xi d\xi$. Using the equation (5.23), one can calculate the following terms as below

$$w_1 = (-\frac{1}{24}\alpha^2\mu^2\omega^2\xi^4 + \frac{1}{24}\omega^2\xi^4)A_0 + (-\frac{1}{12}\mu^2\omega^2\alpha\xi^4 - \frac{1}{120}\alpha^2\mu^2\omega^2\xi^5 + \\ \frac{1}{120}\omega^2\xi^5)A_1 + (-\frac{1}{24}\mu^2\omega^2\xi^4 - \frac{1}{24}\alpha^2\xi^4 - \frac{1}{60}\mu^2\omega^2\alpha\xi^5 - \frac{1}{720}\alpha^2\mu^2\omega^2\xi^6 + \\ \frac{1}{720}\omega^2\xi^6)A_2 + (-\frac{1}{12}\alpha\xi^4 - \frac{1}{120}\mu^2\omega^2\xi^5 - \frac{1}{120}\alpha^2\xi^5 - \frac{1}{360}\mu^2\omega^2\alpha\xi^6 \\ -\frac{1}{5040}\alpha^2\mu^2\omega^2\xi^7 + \frac{1}{5040}\omega^2\xi^7)A_3, \tag{5.24}$$

and

$$w_2 = (-\frac{1}{60}\alpha\omega^2\xi^5 - \frac{1}{720}\mu^2\omega^2\xi^6 - \frac{1}{720}\alpha^2\omega^2\xi^6 + ...)A_0 \\ +(-\frac{1}{360}\alpha\omega^2\xi^6 - \frac{1}{5040}\mu^2\omega^2\xi^7 - \frac{1}{5040}\alpha^2\omega^2\xi^7 + ...)A_1 \\ +(-\frac{1}{2520}\alpha\omega^2\xi^7 + \frac{1}{720}\mu^4\omega^4\xi^6 - \frac{1}{20160}\mu^2\omega^4\xi^8 + ...)A_2 \\ +(-\frac{1}{10080}\alpha\omega^2\xi^8 + \frac{1}{5040}\mu^4\omega^4\xi^7 - \frac{1}{181440}\mu^2\omega^4\xi^9 + ...)A_3. \tag{5.25}$$

Here, w_0, w_1, w_2 present three terms of the series. The accuracy of this calculation depends on the number of terms. For achieving good accuracy, 40 terms of this series have been calculated. Applying the boundary conditions (5.18, 5.19) or any set of (2.13-2.16), w series can be presented in matrix form as below

$$[M(\omega)][A] = 0. \tag{5.26}$$

The natural frequency of the nanobeam is calculated from the equation (5.26).

5.4. Results and discussion

In this section, the efficiency of the homotopy perturbation method for solving the transverse vibration problems of tapered nanobeams with elastic supports is demonstrated. This study can be described by the following steps. First of all, the results of the present paper are examined and compared with the results of

published papers in the literature. Secondly, frequency in different modes of the presented model is illustrated in tabular form for rigid boundary supports. Thirdly, frequency ratio versus taper ratio for different supports are presented graphically. Finally, the mode shapes of the nanobeam are presented for different values of the taper ratio.

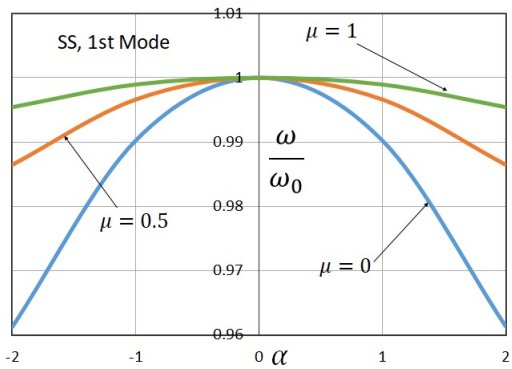

Figure 13. Frequency ratio versus taper ratio (first mode, SS)

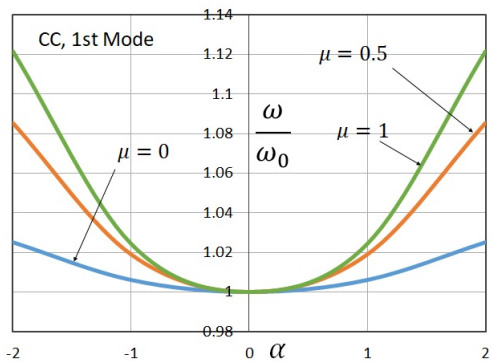

Figure 14. Frequency ratio versus taper ratio (first mode, CC)

In Table 7, obtained frequencies of the present tapered nanobeam are also compared with the frequencies of a regular nanobeam. For this comparison, taper ratio $\alpha = 0$ is considered in the present study. Obtained results show good agreement with the results of Phadikar and Pradhan [60]. On the other hand, in Table 8, the natural frequencies of tapered nanobeams obtained in the present study are compared with the natural frequencies of the tapered macro beam. For this comparison, the nonlocal parameter $\mu = 0$ is considered. The results obtained in the present study show very good agreement with the results of Mao and Pietrzko [56]. Table 9 describes the natural frequency of tapered nanobeams with different rigid supports. It is clear from this table that frequency decreases with the increase of the nonlocal parameter. On the other hand, the effect of taper ratio on the frequency depends on the end support system.

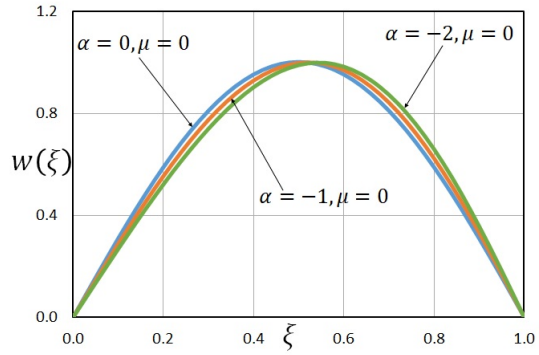

Figure 15. Mode shape for different taper ratios (SS, first mode)

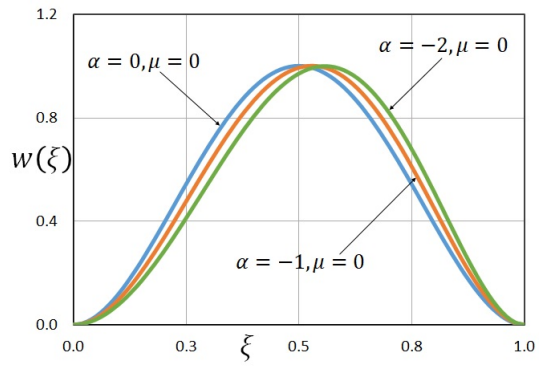

Figure 16. Mode shape for different taper ratios (CC, first mode)

Table 7. Data comparision with the regular (uniform) nanobeam

Boundary	Method	δ	μ	frequency (ω)		
				1	2	3
SS	[60]	0	1	2.9936	6.2061	9.3796
	Present	0	1	2.9934	6.2055	9.3725
CC	[60]	0	1	6.0574	8.9011	12.4822
	Present	0	1	6.0561	8.8950	12.4521

Table 8. Data comparision with the macro tapered beam

Boundary	Method	δ	μ	frequency (ω)			
SS				1	2	3	4
	[56]	0	0	9.86960	39.47841	88.82643	157.9136
	Present	0	0	9.87011	39.48046	88.82031	157.9218
	[56]	-1	0	9.77291	39.57036	88.97052	158.0841
	Present	-1	0	9.77246	39.57421	88.97656	158.0781
	[56]	-2	0	9.48725	39.85231	89.40520	158.5968
	Present	-2	0	9.48681	39.85546	89.39843	158.6093

Table 9. Natural frequency of the tapered nanobeam with different rigid supports

		SS			CC		
μ	α	1	2	3	1	2	3
0	0	9.87011	39.4804	88.8203	22.3722	61.6718	120.898
1	0	2.99340	6.20556	9.37255	6.05615	8.89501	12.4521
2	0	1.55126	3.13183	4.70585	3.11230	4.48164	6.26835
0	-1	9.77324	39.5675	88.9765	22.5103	61.8607	121.109
1	-1	2.99013	6.21035	9.37421	6.20361	8.79931	12.6028
2	-1	1.55087	3.13261	4.70585	3.19345	4.42382	6.37382
0	-2	9.48671	39.8530	89.3984	22.9366	62.4199	121.725
1	-2	2.97988	6.22773	9.37734	6.79335	8.34355	12.8320
2	-2	1.54931	3.13496	4.70664	3.55449	4.12416	6.48007

Figures 13, and 14 illustrate frequency ratio versus taper ratio for different values of the nonlocal parameter at simply supported and clamped nanobeams. The frequency ratio is calculated from the frequency of the tapered beam and the frequency of the regular beam for three different values of the nonlocal parameter. The frequency ratio shows different patterns for different support systems. It is clear that the sign of taper ratio is not effective in the case of simply supported and clamped nanobeams.

Figures 15, and 16 illustrate the shape mode of simply supported and fully clamped tapered nanobeams, respectively. It is clear from these figures that the increase in the value of the taper ratio increases the variation of the mode shape.

6. NATURAL VIBRATION OF AXIALLY GRADED MULTI CRACKED NANOBEAMS IN THERMAL ENVIRONMENT USING POWER SERIES

In this section, a numerical investigation of the dynamic characteristics of axially graded multi cracked nanobeams in a thermal environment is demonstrated by applying the power series solution technique (see Hossain and Lellep [36]).

6.1. Description of the problem

The geometry of an axially graded multi-cracked nanobeam is illustrated in Figure 17. The left endpoint of the beam is located at the origin of the coordinate system. The neutral axis of the beam overlaps with the x-axis and the height of the beam is placed along the z-axis. Here, L, b, h describe the length, width and height of the beam, respectively. Multiple open cracks are considered at the distance of a_i to a_n from the left endpoint. The material of the beam is axially graded along the x-axis. E and ρ are the elasticity and density varying exponentially from one end to another end. The objective of this analysis is to examine the natural vibration of the axially graded multi cracked nanobeam.

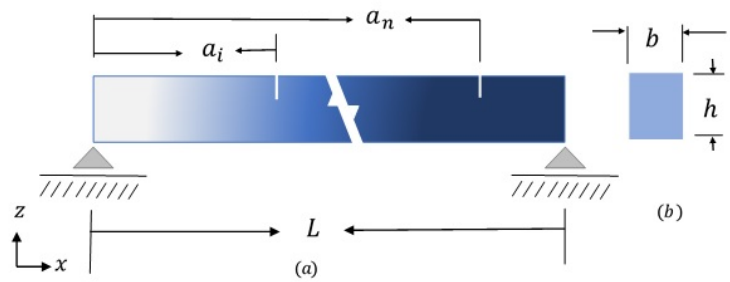

Figure 17. (a) An axially graded multi-cracked nanobeam, (b) Cross-section of the beam

6.2. Mathematical model

6.2.1. Derivation of the governing equation

In this paper, the beam is axially graded and also subjected to thermal load. Therefore, the material properties such as elasticity and density (2.33) are varying along the x-axis. Similarly, the thermal load (2.34) is also varying with the elasticity as an axial load. Considering these variations, and combination of equations (2.7)

and (2.10) can be expressed as

$$\begin{aligned}\frac{\partial^2}{\partial x^2}(E(x)I\frac{\partial^2 W}{\partial x^2}) - (e_0a)^2\frac{\partial^2}{\partial x^2}[\rho(x)A\frac{\partial^2 W}{\partial t^2} - \frac{\partial}{\partial x}(N(x)\frac{\partial W}{\partial x})] \\ -\frac{\partial}{\partial x}(N(x)\frac{\partial W}{\partial x}) + \rho(x)A\frac{\partial^2 W}{\partial t^2} = 0.\end{aligned} \tag{6.1}$$

Using the transformation (2.11) and non-dimensional parameters (2.12) and applying the axially graded material properties (2.33), the equation (6.1) can be expressed as

$$\begin{aligned}(\lambda^2\frac{d^2w}{d\xi^2} + 2\lambda\frac{d^3w}{d\xi^3} + \frac{d^4w}{d\xi^4}) + \mu^2\omega^2(\lambda^2 w + 2\lambda\frac{dw}{d\xi} + \frac{d^2w}{d\xi^2}) \\ -\mu^2 n(\lambda^3\frac{dw}{d\xi} + 3\lambda^2\frac{d^2w}{d\xi^2} + 3\lambda\frac{d^3w}{d\xi^3} + \frac{d^4w}{d\xi^4}) + n(\frac{dw}{d\xi} + \frac{d^2w}{d\xi^2}) - \omega^2 w = 0,\end{aligned} \tag{6.2}$$

here, λ is the parameter of non-homogeneity, n indicates the dimensionless thermal load. Therefore, the equation (6.2) can be presented in a simplified form as

$$\frac{d^4w}{d\xi^4} + \beta_1\frac{d^3w}{d\xi^3} + \beta_2\frac{d^2w}{d\xi^2} + \beta_3\frac{dw}{d\xi} + \beta_4 w = 0, \tag{6.3}$$

where

$$\begin{aligned}\beta_1 = \frac{2\lambda - 2\lambda\mu^2 n}{1-\mu^2 n},\ \ \beta_2 = \frac{\lambda^2 + \mu^2\omega^2 - 3\mu^2 n\lambda^2 + n}{1-\mu^2 n}, \\ \beta_3 = \frac{2\mu^2\omega^2\lambda - \mu^2 n\lambda^3 + n}{1-\mu^2 n},\ \ \beta_4 = \frac{\mu^2\omega^2\lambda^2 - \omega^2}{1-\mu^2 n}.\end{aligned}$$

In this nanobeam, multiple cracks are considered where n number of cracks separate the beam into $n+1$ segments. Finally, the governing equations for $n+1$ number of segments can be expressed as

$$\frac{d^4w_i}{d\xi^4} + \beta_1\frac{d^3w_i}{d\xi^3} + \beta_2\frac{d^2w_i}{d\xi^2} + \beta_3\frac{dw_i}{d\xi} + \beta_4 w_i = 0, \tag{6.4}$$

where $i = 1,2,3,...,n+1$. These equations (6.4) represent the set of governing equations considering the $n+1$ segments that are separated at the location of cracks a_j, where $j = 1,2,...,n$. One can solve these equations (6.4) by applying in-between conditions (2.31) at the crack locations and any one set of end conditions (2.13-2.16) for the boundary supports.

6.3. Power series solution

The power series solution technique is very useful to solve linear and nonlinear problems. The governing equation can be solved using the power series solution technique. Using the rules of power series (2.48-2.50), one can replace the

derivatives of deflection in the governing equation (6.4). Therefore, simplifying the equation can be written as

$$\begin{aligned} A_{k+4} = &-\frac{\beta_1}{(k+4)}A_{k+3} - \frac{\beta_2}{(k+4)(k+3)}A_{k+2} \\ &-\frac{\beta_3}{(k+4)(k+3)(k+2)}A_{k+1} - \frac{\beta_4}{(k+4)(k+3)(k+2)(k+1)}A_k, \end{aligned} \tag{6.5}$$

here, $A_{k+4}, A_{k+3}, ..., A_k$ are the power series coefficients. Using the above relation in the equation (6.5), one can calculate the series coefficients as follows

$$\begin{aligned} A_4 &= -\frac{1}{4}\beta_1 A_3 - \frac{1}{12}\beta_2 A_2 - \frac{1}{24}\beta_3 A_1 - \frac{1}{24}\beta_4 A_0, \\ A_5 &= \frac{1}{20}(\beta_1^2 - \beta_2)A_3 + \frac{1}{60}(\beta_1\beta_2 - \beta_3)A_2 \\ &\quad + \frac{1}{120}(\beta_1\beta_3 - \beta_4)A_1 + \frac{1}{120}\beta_1\beta_4 A_0, \\ A_6 &= -\frac{1}{120}(\beta_1^3 - 2\beta_1\beta_2 + \beta_3)A_3 - \frac{1}{360}(\beta_1^2\beta_2 - \beta_1\beta_3 - \beta_2^2 + \beta_4)A_2 \\ &\quad -\frac{1}{720}(\beta_1^2\beta_3 - \beta_1\beta_4 - \beta_2\beta_3)A_1 - \frac{1}{720}(\beta_1^2\beta_4 - \beta_2\beta_4)A_0. \end{aligned} \tag{6.6}$$

Applying the series coefficients, the solution for each segment of the beam can be written as

$$w_i = A_{i,0} + A_{i,1}\xi + A_{i,2}\xi^2 + A_{i,3}\xi^3 + \sum_{k=4}^{\infty} A_{i,k}\xi^k, \tag{6.7}$$

where $i = 1, 2, ..., n+1$. Using the simply-supported boundary conditions (2.13) and intermediate conditions for the crack (2.31), one can eliminate constant coefficients ($A_{i,k}$) and solve these equations to form a matrix as follows

$$\begin{bmatrix} m_{1,1} & \dots & \dots & m_{1,4(n+1)} \\ \dots & \dots & \dots & \dots \\ \dots & \dots & \dots & \dots \\ m_{4(n+1),1} & \dots & \dots & m_{4(n+1),4(n+1)} \end{bmatrix} \begin{bmatrix} A_{1,0} \\ \dots \\ \dots \\ A_{(n+1),3} \end{bmatrix} = 0, \tag{6.8}$$

here, $m_{1,1}$, ..., $m_{4(n+1),4(n+1)}$ indicate the elements of the matrix. The value of natural frequency for the multi-cracked nanobeam can be determined by solving the above matrix equation (6.8). In this section, single, double, and triple cracked nanobeams are analyzed.

6.4. Numerical results and discussion

In this section, parametric analysis is performed to scrutinize their impacts on the natural frequency of the axially graded multi cracked nanobeam in a thermal environment. First of all, the efficiency of the solution technique is examined by

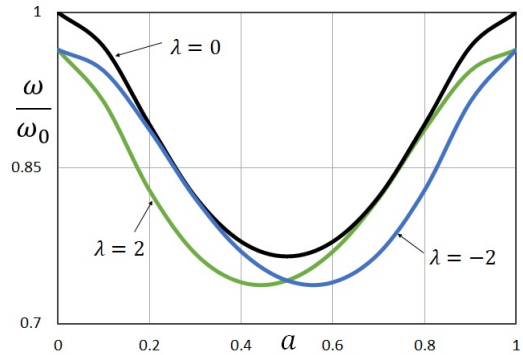

Figure 18. Frequency ratio versus crack position (SS, first mode)

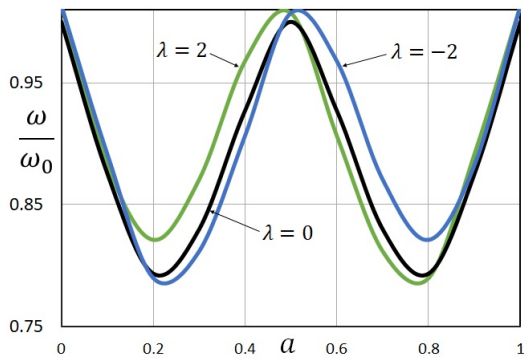

Figure 19. Frequency ratio versus crack position (SS, second mode)

comparing the obtained results with the results of relevant papers in the existing literature. In addition, the influences of crack position on the various modes of natural frequency for several values of the gradient parameter are studied and presented graphically. Moreover, the effects of temperature, non-homogeneity, and the nonlocal parameter on the natural frequency are presented in tabular forms. Finally, the mode shapes are depicted to investigate the axially graded multi cracked nanobeam and to study the effects of crack severity on the transverse deflection.

6.4.1. Comparison of results

In this section, the outcomes of the study are compared with the outcomes of some benchmark research in the existing literature. This comparison is performed by investigating the effects of nonlocal parameter (μ), thermal load (n), and crack severity on different modes of the natural frequency. In Table 10, the first mode of natural frequency (square root) for simply supported nanobeams is presented. The effect of cracks is not considered as well as the beam is considered uniform and homogeneous in this section of calculation. Different values of nonlocal parameter (μ) and thermal load (n) are considered. It is understandable from this

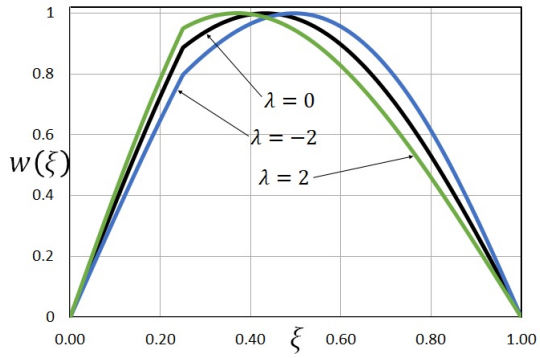

Figure 20. Mode shape for different values gradient parameter (first mode, SS)

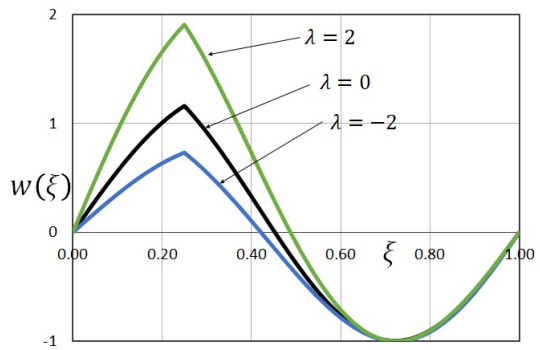

Figure 21. Mode shape for different values gradient parameter (second mode, SS)

tabular data that the natural frequency decreases with the increase of the nonlocal parameter. Therefore, the natural frequency increases for the decrease of temperature. Outcomes are verified by the results of Esen et al. [20] and Aria et al. [6]. In Table 11, different modes of natural frequency for a double cracked beam with different values of the nonlocal parameter and crack severity are studied. Two cracks in the beam are located at $a_1 = 0.3$ and $a_2 = 0.7$, respectively. It is obvious from this tabular data that frequency decreases with the increase of the nonlocal parameter. Values of frequency are also influenced by the crack severity. This table data are also compared with the results of Roostai and Haghpanahi [66]. This comparison shows a close match among these results. Similarly, in Table 12, different modes of natural frequency (square root) for the simply supported single cracked nanobeam are demonstrated. Non-homogeneity of nanobeams is ignored in this section of calculation. Different values of crack positions (a), crack severity (K), nonlocal parameter (μ) are also considered. It is comprehensible from this tabular data that the natural frequency decreases with the increase of crack severity. Frequency shows the lower value at the crack position of $a = 0.5$ than $a = 0.25$. This table data also match with the results of Esen et al. [20] and Aria et al. [6]. These evaluations show a good agreement between current data and the data of other researchers.

6.4.2. Effect of crack locations

The location of the crack is also crucial as like as the crack severity for analyzing the cracked beam. In Figures 18, 19, first modes of frequency for simply supported nanobeams are demonstrated. Thermal load is ignored in this section of the calculation. The frequency ratio is calculated by the frequency at any point with non-homogeneity and the frequency at the initial point without considering non-homogeneity. In this section, nonlocal parameter $\mu = 0.1$ and crack severity $K = 0.35$ are applied. It is evident from these figures that in the case of simply supported and the first mode of frequency, the frequency ratio slightly decreases for the presence of non-homogeneity. However, in other cases, frequency increases with the presence of non-homogeneity. It is very important in these curves that the frequency ratio is not affected by the positive or negative sign of non-homogeneity. The effect of crack location is also influenced by the end support systems.

6.4.3. Frequency for axially graded intact and cracked nanobeams under thermal load

In this section, Tables 13, and 14 represent the effect of temperature on the natural frequency for axially graded intact or cracked nanobeams, respectively. Interactions between temperature, non-homogeneity, nonlocal parameter, end supports, and different modes of frequency of intact and cracked nanobeams are very diverse. Table 13 represents the relationship between the nonlocal parameter,

Table 10. Natural frequency (square root) for varying nonlocal parameter, thermal load and different end supports

SS	$\mu = 0$			$\mu = 0.1$		
n	Present	[20]	[6]	Present	[20]	[6]
2	2.9688	2.9672	2.9680	2.8815	2.8810	2.8800
1	3.0589	3.0575	3.0563	2.9793	2.9791	2.9787
0	3.1416	3.1416	3.1415	3.0684	3.0683	3.0680
-1	3.2184	3.2173	3.2180	3.1505	3.1504	3.1501
-2	3.2901	3.2896	3.2894	3.2268	3.2266	3.2262

Table 11. Natural frequency for the double cracked beam with different values of nonlocal parameter and crack severity

		SS			
		K=0.0325		K=0.075	
μ	Mode	[66]	Present	[66]	Present
0	1	9.474	9.475	9.023	9.023
	2	37.335	37.338	34.986	34.986
	3	88.313	86.383	87.741	85.883
1	1	2.873	2.873	2.732	2.732
	2	5.858	5.858	5.46	5.459
	3	9.313	9.313	9.236	9.236

thermal load, and non-homogeneity in absence of cracks. In this section, three different values of the nonlocal parameter, thermal load from -2 to 2 and non-homogeneity -2 to 2 are considered. It is very clear that the frequency decreases for the increase of the nonlocal parameter. On the other hand, frequency increases with the decrease of temperature. Table 14 represents the relationship between the nonlocal parameter, thermal load and non-homogeneity in the presence of a crack. In this section, different values of nonlocal parameter, thermal load and non-homogeneity are considered as in Table 13. In addition, a crack is considered at crack location $a = 0.25$ with the crack severity $K = 0.35$. The relationship between thermal load, non-homogeneity, and natural frequency becomes more changeable in the presence of cracks for various modes of frequency. In Table 15, the natural frequency for a triple cracked beam with several values of the nonlocal parameter and crack severity is demonstrated. Three specific cracks are considered at the position of $a_1 = 0.3$, $a_2 = 0.5$, $a_3 = 0.7$, respectively. The effects of non-homogeneity and temperature are not considered. It is understandable in this tabular data that the frequency decreases with the increase of the value of the nonlocal parameter and crack severity.

Table 12. Natural frequency (square root) for the simply supported cracked nanobeam in different mode with varying nonlocal parameter

a	K	mode	$\mu = 0.0$			$\mu = 0.2$		
			Present	[20]	[6]	Present	[20]	[6]
0.5	0	1	3.1416	3.1413	3.1409	2.8908	2.8907	2.8907
		2	6.2833	6.2830	6.2818	4.9582	4.9580	4.9578
	0.35	1	2.7496	2.7493	2.7489	2.5232	2.5232	2.5232
		2	6.2833	6.2825	6.2819	4.9582	4.9580	4.9578
0.25	0	1	3.1416	3.1416	3.1409	2.8908	2.8908	2.8908
		2	6.2833	6.2825	6.2818	4.9582	4.9580	4.9580
	0.35	1	2.9072	2.9068	2.9064	2.6646	2.6645	2.6645
		2	5.6491	5.6486	5.6484	4.4168	4.4169	4.4168

Table 13. Frequency for several values of nonlocal parameter, thermal load and nonhomogeneity without crack

SS	$K = 0$						
		$\mu = 0$			$\mu = 0.2$		
n	λ	1	2	3	1	2	3
-2	-2	10.3271	40.7773	90.3672	8.9497	26.4121	43.9336
	0	10.8252	40.4648	89.8203	9.4653	26.1387	43.7070
	2	10.5127	40.8320	90.3984	9.1021	26.4551	43.9570
0	-2	9.48682	39.8555	89.3984	8.1079	24.9785	41.9179
	0	9.87012	39.4805	88.8203	8.3569	24.5839	41.6289
	2	9.48682	39.8555	89.3984	8.1079	24.9785	41.9179
2	-2	8.58057	38.9004	88.4297	7.1704	23.4550	39.8008
	0	8.81396	38.4668	87.8203	7.0796	22.9199	39.4336
	2	8.33545	38.8496	88.3984	6.9741	23.4082	39.7773

6.4.4. Mode shape illustration

Mode shape is one of the important characteristics that explain the vibration of structural components. It describes the transverse displacement from the beam axis during vibration. It is a significant measure that explains the pattern of vibration. In this section, the effects of non-homogeneity on the mode shape of cracked nanobeams are illustrated. In order to understand the dynamic behavior of cracked nanobeams, mode shape analysis is necessary. In Figures (20, 21), different mode shapes of nanobeams are demonstrated where the location of crack $a = 0.25L$, value of the nonlocal parameter $\mu = 0.1$, and crack severity $K = 0.35$ are considered. In this section of calculation, thermal load $n = 1$ is considered. Different values of non-homogeneity $\lambda = 2$, $\lambda = 0$ and $\lambda = -2$ are applied. It is comprehensible from these figures that mode shapes of cracked nanobeam are considerably changed by the non-homogeneity. Variation changes with the change

Table 14. Frequency for several values of nonlocal parameter, thermal load and nonhomogeneity with crack

SS	$K = 0.35, a = 0.25$						
		$\mu = 0$			$\mu = 0.2$		
n	λ	1	2	3	1	2	3
-2	-2	9.1362	32.1699	82.4297	7.7495	20.2324	40.2070
	0	9.2583	32.7246	83.3203	7.9887	20.5723	40.1445
	2	8.6909	33.9824	85.3359	7.4907	21.3496	40.6367
0	-2	8.4341	31.4004	81.5078	7.0942	19.2588	38.4238
	0	8.4517	31.9121	82.3828	7.1001	19.5088	38.3457
	2	7.8081	33.1894	84.3984	6.6812	20.3730	38.9394
2	-2	7.6694	30.6113	80.5859	6.3442	18.2119	36.5410
	0	7.5503	31.0762	81.4297	6.0474	18.3486	36.4394
	2	6.7993	32.3809	83.4765	5.7388	19.3057	37.1426

Table 15. Natural frequency for the triple cracked nanobeam with several values of nonlocal parameter and crack severity

SS	K=0.0325			K=0.075		
μ	1	2	3	1	2	3
0	9.203	37.338	83.977	8.506	34.986	80.523
0.5	4.941	11.306	17.692	4.563	10.542	16.655
1	2.79	5.858	8.992	2.576	5.459	8.459
CC						
0	21.708	58.508	107.492	21.037	55.223	102.602
0.5	10.622	16.247	22.545	10.229	15.138	20.393
1	5.846	8.363	11.522	5.622	7.786	10.405

of the value of non-homogeneity. This variation also increases in the higher mode of frequency.

7. CONCLUDING REMARKS

In this study, the dynamic behavior of nanobeams considering various physical and geometrical properties has been analyzed. Conventional continuum theory and Eringen's nonlocal theory of elasticity have been used to simulate the problem. Several physical properties such as axially graded material and temperature have been considered. In an axially graded beam, material properties such as modulus of elasticity and density vary from one end to another end exponentially. The effect of temperature has been considered uniformly over the beam where the thermal load is accumulated with the mechanical load. Similarly, several geometrical properties such as varying cross-sections and cracks have been considered. The width of the beam is changing exponentially from one end to another end. Single and multiple cracks have been considered where cracks are simulated with the help of the rotational spring model. In this study, a double nanobeam has been analyzed where both beams are connected to each other by the Winkler-type spring model.

The most significant part of this analysis is employing several numerical techniques that are rare in the analyses of the nano-material. These techniques are the homotopy perturbation method, power series solution technique, and Maclaurin series solution technique. These techniques have been successfully applied and the obtained results have been verified with the results of existing literature.

In this study, the frequency of nanobeams decreases with the increase of crack depth. Frequency is affected by the crack location. The effect of crack location is also influenced by the end support systems. In the case of double nanobeams, natural frequency increases if the spring constant increases. The first mode of frequency is less influenced than the higher mode of frequency for the increase of spring constants. In the case of taper and non-homogeneous beams, frequency is affected by the taper ratio and non-homogeneity. The effects of taper ratio and non-homogeneity increase with the increase of the mode of frequency. However, the frequency is not affected by the sign (negative or positive) of the taper ratio and non-homogeneity in simply supported and fully clamped nanobeams. The effect of elastic supports is influenced by the nonlocal parameter and taper ratio. Nonlocal parameter reduces the stiffness of elastic supports. An increase in thermal load decreases frequency. Macrobeams and nanobeams both are similarly affected by the crack severity, taper ratio, non-homogeneity, and temperature.

In this study, a convenient way to depict the mode shape diagram of nanobeams has been presented. Therefore, the dynamic behavior of nanobeams has been illustrated with the aid of the mode shape diagram. It is evident from this analysis that the mode shape of nanobeams is significantly affected by the nonlocal parameter, taper ratio, non-homogeneity, crack severity, and the influence of temperature. Nonetheless, crack is one of the influential factors in changing the mode shape.

BIBLIOGRAPHY

1. N. Abid, A. M. Khan, S. Shujait, K. Chaudhary, M. Ikram, M. Imran, J. Haider, M. Khan, Q. Khan and M. Maqbool, Synthesis of nanomaterials using various top-down and bottom-up approaches, influencing factors, advantages, and disadvantages: A review, Adv. Colloid Interface Sci., **300** 102597 (2022).
2. S. Adhikari, D. Karlicic and X. Liu, Dynamic stiffness of nonlocal damped nano-beams on elastic foundation, Eur. J. Mech. A Solids, **86** 104144 (2021).
3. H. M. E. Afefy, M. H. Mahmoud and T. M. Fawzy, Rehabilitation of defected RC stepped beams using CFRP, Eng. Struct., **49** 295–305 (2013).
4. I. Ahmadi, Vibration analysis of 2D-functionally graded nanobeams using the nonlocal theory and meshless method, Eng. Anal. Bound. Elem., **124** 142–154 (2021).
5. M. Ahmadvand and P. Asadi, Free vibration analysis of flexible rectangular fluid tanks with a horizontal crack, Appl. Math. Model., **91** 93–110 (2021).
6. A. I. Aria, M. I. Friswell and T. Rabczuk, Thermal vibration analysis of cracked nanobeams embedded in an elastic matrix using finite element analysis, Compos. Struct., **212** 118–128 (2019).
7. M. S. Atanasov and V. Stojanovic, Nonlocal forced vibrations of rotating cantilever nano-beams, Eur. J. Mech. A Solids, **79** 103850 (2020).
8. A. Bahrami, A wave-based computational method for free vibration, wave power transmission and reflection in multi-cracked nanobeams, Compos. B. Eng., **120** 168-181 (2017).
9. E. Barkanov, E. Skukis, B. Petitjean, Characterisation of viscoelastic layers in sandwich panels via an inverse technique, J. Sound Vib. **327** 402–412 (2009).
10. R. P. R. Cardoso, A new beam element which blends the Euler-Bernoulli beam theory with idealised transverse shear flows for aircraft structural analysis, Thin-Walled Struct., **157** 107118 (2020).
11. S. S. B. Chinka, S. R. Putti and B. K. Adavi, Modal testing and evaluation of cracks on cantilever beam using mode shape curvatures and natural frequencies, Struct., **32** 1386–1397 (2021).
12. S. N. Chockalingam, M. Nithyadharan and V. Pandurangan, Shear stress distribution in tapered I-beams: Analytical expression and finite element validation, Thin–Walled Struct., **157** 107152 (2020).
13. S. N. Chockalingam, V. Pandurangan and M. Nithyadharan, Timoshenko beam formulation for in-plane behaviour of tapered monosymmetric I-beams: Analytical solution and exact stiffness matrix, Thin-Walled Struct., **162** 107604 (2021).

14. P. Datta, Active vibration control of axially functionally graded cantilever beams by finite element method, Mater. Today: Proc., **44** 2543–2550 (2021).
15. M. C. Ece, M. Aydogdu and V. Taskin, Vibration of a variable cross-section beam, Mech. Res. Commun., **34** 78–84 (2007).
16. M. A. Eltaher, A. E. Alshorbagy and F. F. Mahmoud, Vibration analysis of Euler–Bernoulli nanobeams by using finite element method, Appl. Math. Model., **37** 4787–4797 (2013).
17. M.A. Eltaher, F.F. Mahmoud, A.E. Assie, E.I. Meletis, Coupling effects of nonlocal and surface energy on vibration analysis of nanobeams, Appl. Math. Comput., **224** 760–774 (2013).
18. A. C. Eringen, Nonlocal Continuum Field Theories, Springer-Verlag NewYork, Inc., New York City, United States (2002).
19. U. Eroglu and E. Tufekci, Exact solution based finite element formulation of cracked beams for crack detection, Int. J. Solids Struct., **96** 240–253 (2016).
20. I. Esen, C. Özarpa and M. A. Eltaher, Free vibration of a cracked FG microbeam embedded in an elastic matrix and exposed to magnetic field in a thermal environment, Compos. Struct., **261** 113552 (2021).
21. S. A. Faghidian, Integro-differential nonlocal theory of elasticity, Int. J. Eng. Sci., **129** 96–110 (2018).
22. S. A. Faghidian, Higher–order nonlocal gradient elasticity: A consistent variational theory, Int. J. Eng. Sci. **154** 103337 (2020).
23. S. H. Hashemi, M. Fakher, R. Nazemnezhad and M. H. S. Haghighi, Dynamic behavior of thin and thick cracked nanobeams incorporating surface effects, Compos. B. Eng., **61** 66–72 (2014).
24. S. M. Hasheminejad, B. Gheshlaghi , Y. Mirzaei and S. Abbasion, Free transverse vibrations of cracked nanobeams with surface effects, Thin Solid Films, **519** 2477–2482 (2011).
25. J. H. He, Homotopy perturbation technique, Comput. Methods Appl. Mech. Eng., **178** 257-262 (1999).
26. J. H. He, A coupling method of a homotopy technique and a perturbation technique for non-linear problems, Int. J. Non Linear Mech., **35** 37-43 (2000).
27. J. H. He, Homotopy perturbation method: a new nonlinear analytical technique, Appl. Math. Comput., **135** 73–79 (2003).
28. M. Hossain and J. Lellep, Natural vibrations of nanostrips with cracks, Acta Comment. Univ. Tartu. Math., **25(1)** 87–105 (2021).
29. M. Hossain and J. Lellep, Thermo mechanical vibration of single wall carbon nanotube partially embedded into soil medium, Agron. Res., **19(S1)** 777–787 (2021).

30. M. Hossain, J. Lellep, Effect of temperature on dynamic behavior of cracked metallic and composite beam, Vibroengineering Procedia, **32** 172–178 (2020).
31. M. Hossain and J. Lellep, Natural vibration of stepped nanoplate with crack on an elastic foundation, IOP Conf. Series: Materials Science and Engineering, **660** 012051 (2019).
32. M. Hossain and J. Lellep, Transverse vibration of tapered nanobeam with elastic supports, Eng. Res. Express, **3(1)** 015019 (2021).
33. M. Hossain and J. Lellep, The effect of rotatory inertia on natural frequency of cracked and stepped nanobeam, Eng. Res. Express, **2(3)** 035009 (2020).
34. M. Hossain and J. Lellep, Mode shape analysis of dynamic behaviour of cracked nanobeam on elastic foundation, Eng. Res. Express, **3(4)** 045003 (2021).
35. M. Hossain and J. Lellep, Analysis of free vibration of tapered cracked double nanobeams using Maclaurin series, Eng. Res. Express, **4(2)** 025034 (2022).
36. M. Hossain and J. Lellep, Natural vibration of axially graded multi cracked nanobeam in thermal environment using power sereis, J. Vib. Eng. Technol., https://doi.org/10.1007/s42417-022-00555-3, (2022).
37. M. H. Hsu, Vibration analysis of edge-cracked beam on elastic foundation with axial loading using the differential quadrature method, Comput. Methods Appl. Mech. Eng. **194** 1-17 (2005).
38. Z. Kala, Estimating probability of fatigue failure of steel structures, Acta Comment. Univ. Tartu. Math., **23(2)** (2019).
39. M. K. Kalkowski, J. M. Muggleton and E. Rustighi, An experimental approach for the determination of axial and flexural wavenumbers in circular exponentially tapered bars, J. Sound Vib., **390** 67–85 (2017).
40. B. Karami and M. Janghorban, A new size-dependent shear deformation theory for free vibration analysis of functionally graded/anisotropic nanobeams, Thin-Walled Struct., **145** 106-227 (2019).
41. L. L. Ke and Y. S. Wang, Free vibration of size-dependent magneto-electro-elastic nanobeams based on the nonlocal theory, Phys. E, **63** 52-61 (2014).
42. R. Kumar and S. K. Singh, Crack detection near the ends of a beam using wavelet transform and high resolution beam deflection measurement, Eur. J. Mech. A Solids, **88** 104259 (2021).
43. J. Lellep and A. Lenbaum, Free vibrations of stepped nano-beams, Int. J. Comput. Methods Exp. Meas., **6(4)** (2018).
44. J. Lellep and A. Lenbaum, Natural vibrations of stepped nanobeams with defects, Acta Comment. Univ. Tartu. Math., **23(1)** (2019).
45. S. Li and G. Wang, Introduction to micromechanics and nanomechanics, World scientific Publishing Co. Pte. Ltd., Singapore (2008).

46. Z. M. Li and T. Liu, A new displacement model for nonlinear vibration analysis of fluid-conveying anisotropic laminated tubular beams resting on elastic foundation, Eur. J. Mech. A Solids, **86** 104172 (2021).
47. Z. Li, Z. Song, W. Yuan and X. He, Axially functionally graded design methods for beams and their superior characteristics in passive thermal buckling suppressions, Compos. Struct., **257** 113390 (2021).
48. Z. Li, Y. Xu and D. Huang, Analytical solution for vibration of functionally graded beams with variable cross-sections resting on Pasternak elastic foundations, Int. J. Mech. Sci., **191** 106084 (2021).
49. G. Li, Y. Xing, Z. Wang and Q. Sun, Effect of boundary conditions and constitutive relations on the free vibration of nonlocal beams, Results Phys., **19** 103414 (2020).
50. J. Li, T. Wang, X. Liu, B. Chen, Q. Xu, C. Wang and Y. Li, Double-beam modeling and experiments of resonance behaviors of AFM-based nanowires, Int. J. Mech. Sci., **213** 106867 (2022).
51. M. Loghmani and M. R. H. Yazdi, An analytical method for free vibration of multi cracked and stepped nonlocal nanobeams based on wave approach, Results Phys., **11** 166–181 (2018).
52. M. A. Mahmoud, Natural frequency of axially functionally graded, tapered cantilever beams with tip masses, Eng. Struct., **187** 34–42 (2019).
53. S. Malik, D. K. Singh, G. Bansal, V. Paliwal and A. R. Manral, Finite element analysis of Euler's Bernoulli cantilever composite beam under uniformly distributed load at elevated temperature, Materials Today: Proceedings, **46** 10725–10731 (2021).
54. M. Malik and D. Das, Free vibration analysis of rotating nano-beams for flap-wise, chord-wise and axial modes based on Eringen's nonlocal theory, Int. J. Mech. Sci., **179** 105655 (2020).
55. A. E. Mamaghani, H. Sarparast and M. Rezaei, On the vibrations of axially graded Rayleigh beams under a moving load, Appl. Math. Model., **84** 554–570 (2020).
56. Q. Mao and S. Pietrzko, Free vibration analysis of a type of tapered beams by using Adomian decomposition method, Appl. Math. Comput., **219** 3264–3271 (2012).
57. B. Martin and A. Salehian, Techniques for approximating a spatially varying Euler-Bernoulli model with a constant coefficient model, Appl. Math. Model., **79** 260–283 (2020).
58. S. E. Motaghiana, M. Mofida, P. Alanjari, Exact solution to free vibration of beams partially supported by an elastic foundation, Sci. Iran. A, **18(4)** 861–866 (2011).
59. Z. Ni and H. Hua, Axial-bending coupled vibration analysis of an axially-loaded stepped multi-layered beam with arbitrary boundary conditions, Int.

J. Mech. Sci., **138–139** 187–198 (2018).

60. J. K. Phadikar and S. C. Pradhan, Variational formulation and finite element analysis for nonlocal elastic nanobeams and nanoplates, Comput. Mater. Sci., **49** 492–499 (2012).
61. Q. H. Pham, V. K. Tran, T. T. Tran, T. N. Thoi, P. C. Nguyen, V. D. Pham, A nonlocal quasi-3D theory for thermal free vibration analysis of functionally graded material nanoplates resting on elastic foundation, Case Stud. Therm. Eng., **25** 101170 (2021).
62. R. Prasad and A. Banerjee, Influence of conicity on the free wave propagation in symmetric tapered periodic beam, Mech. Res. Commun., **111** 103655 (2021).
63. S. Rajasekaran and H. B. Khaniki, Bending, buckling and vibration of small-scale tapered beams, Int. J. Eng. Sci., **120** 172-188 (2012).
64. S. Rajasekaran and H. B. Khaniki, Size-dependent forced vibration of non-uniform bi-directional functionally graded beams embedded in variable elastic environment carrying a moving harmonic mass, Appl. Math. Model., **72** 129–154 (2019).
65. J. N. Reddy, Theory and analysis of elastic plates and shells, Taylor and Francis Group CRC press, Boca Raton, Florida (2007).
66. H. Roostai and M. Haghpanahi, Vibration of nanobeams of different boundary conditions with multiple cracks based on nonlocal elasticity theory, Appl. Math. Model., **38** 1159–1169 (2014).
67. M. A. D. Rosa and M. Lippiello, Closed-form solutions for vibrations analysis of cracked Timoshenko beams on elastic medium: An analytically approach, Eng. Struct., **236** 111946 (2021).
68. S. Šalinić, A. Obradović and A. Tomović, Free vibration analysis of axially functionally graded tapered, stepped, and continuously segmented rods and beams, Compos. B. Eng., **150** 135–143 (2018).
69. M. S. Sari,W. G. Al-Kouz and A. M. Atieh, Transverse Vibration of Functionally Graded Tapered Double Nanobeams Resting on Elastic Foundation, Appl. Sci., **10** 493 (2020).
70. M. Simsek, Nonlinear free vibration of a functionally graded nanobeam using nonlocal strain gradient theory and a novel Hamiltonian approach, Int. J. Eng. Sci., **105** 12–27 (2016).
71. M. Soltani, B. Asgarian and F. Mohri, Elastic instability and free vibration analyses of tapered thin-walled beams by the power series method, J. Constr. Steel Res., **96** 106–126 (2014).
72. M. Song, Y. Gong, J. Yang, W. Zhu and S. Kitipornchai, Nonlinear free vibration of cracked functionally graded graphene platelet-reinforced nanocomposite beams in thermal environments, J. Sound Vib., **468** 115115 (2020).

73. Z. Su, G. Jin and T. Ye, Vibration analysis of multiple-stepped functionally graded beams with general boundary conditions, Compos. Struct., **186** 315–323 (2018).
74. A. S. Surla, S. Y. Kang and J. S. Park, Inelastic buckling assessment of monosymmetric I-beams having stepped and non-compact flange sections, J. Constr. Steel Res., **114** 325–337 (2015).
75. S. Sushobhan and L. Khazanovich, A self-contained element for modeling crack propagation in beams, Eng. Fract. Mech., **242** 107460 (2021).
76. H. Tada, P. Paris and G. Irwin, the stress analysis of crack hand book, Del Research corporation, Hellerlown, Pennsylvania (1973).
77. J. H. Wan, S. W. Liu, X. Y. Li, L. M. Zhang and H. P. Zhao, Buckling analysis of tapered piles using non-prismatic beam-column element model, Comput. Geotech., **139** 104370 (2021).
78. Q. Wu, S. Guo, X. Li and G. Gao, Crack diagnosis method for a cantilevered beam structure based on modal parameters, Meas. Sci. Technol., **31** 035001 (2020).
79. Y. Yan, B. Liu, Y. Xing, E. Carrera and A. Pagani, Free vibration analysis of variable stiffness composite laminated beams and plates by novel hierarchical differential quadrature finite elements, Compos. Struct., **274** 114364 (2021).
80. S. Yin, Z. Xiao and Y. Deng, G. Zhang, J. Liu and S. Gu, Isogeometric analysis of size-dependent Bernoulli–Euler beam based on a reformulated strain gradient elasticity theory, Comput. Struct., **253** 106577 (2021).
81. Y. F. Zhang, Y. Niu and W. Zhang, Nonlinear vibrations and internal resonance of pretwisted rotating cantilever rectangular plate with varying cross-section and aerodynamic force, Eng. Struct., **225** 111259 (2020).
82. X. Zhang, Z. Ye and Y. Zhou, A Jacobi polynomial based approximation for free vibration analysis of axially functionally graded material beams, Compos. Struct., **225** 111070 (2019).

Summary

In this dissertation, an analysis of the dynamic behavior of nanobeams with different physical and geometrical properties using several numerical techniques is presented. Euler-Bernoulli beam theory and nonlocal theory of elasticity are used to simulate the nanobeam.

Nanobeams are considered with some special requirements such as tapered, axially graded, and double beams. First of all, in a tapered beam, the width of the beam is varying exponentially along the x-axis from one end to another end. The properties of the tapered beam are to reduce material consumption and provide the cross-sectional area according to the moment distribution. Secondly, in an axially graded beam, material properties such as elasticity and density are varying exponentially from one end to another end. The axially graded beam can be considered as a non-homogeneous as well as a composite beam. In this beam, the material properties can be distributed according to the requirement. The axially graded beam overcomes the limitation of conventional composite. Finally, in a double beam, two identical nanobeams are connected by a Winkler-type spring layer. Double beams are used for absorbing the vibration. It reduces deflection and vibration. The double beam is modeled by the coupled differential governing equations.

Some adverse effects such as cracks and the influence of the temperature are considered. Cracks are common defects in nanostructures. Single and multiple cracks are considered in this analysis. According to the model, the crack is replaced by a rotational spring where the crack divides the beam into two segments that are connected to each other by the spring at the crack position. Cracks reduce the overall stiffness of the beam. The effect of temperature is significant for the vibration of nanobeams. The thermal load is compatible with the mechanical load where the thermal load is modeled as an axial load. It reduces the natural frequency.

The main objective of this research is to find suitable techniques for a reliable, cost-effective design that is able to fulfill the desired requirements. That is why the important feature of this research is to apply numerical techniques for solving these problems. Three different approximation techniques such as homotopy perturbation technique, power series method, and Maclaurin series method are used for solving these problems. These techniques are useful for solving linear and non-linear differential equations. However, these techniques are rare to analyze the nano-material. These techniques are applied effectively to scrutinize the model of nanobeams. Obtained results are verified with the results of other researchers in the existing literature. This analysis can be used to design nano-electromechanical devices effectively.

SUMMARY IN ESTONIAN

Nanotalade võnkumise numbriline analüüs

Käesolevas väitekirjas uuritakse nanomaterjalist valmistatud talade omavõnkumisi mitmesuguste kinnitusviiside korral. Väitekirjas on välja töötatud meetodid nanotalade omavõnkesageduse määramiseks astmelise nanotala jaoks erinevate kinnitustingimuste korral; kusjuures astmete nurkades asuvad stabiilsed praod või prao-tüüpi defektid. Prao mõju võnkesagedusele modelleeritakse nn kaalutu väändevedru meetodil. Selle meetodi kohaselt tuleb reaalne astmega tala asendada kahest elemendist koosneva süsteemiga, kus elemendid on omavahel ühendatud väändevedruga, mille jäikus on pöördvõrdeline pinge intensiivsuse koefitsiendiga prao tipu juures. Kuna pinge intensiivsuse koefitsiendi väärtused on leitavad kataloogidest, siis see meetod võimaldab omavahel siduda nanotala omavõnkesageduse ning prao pikkuse ja laiuse.

Väitekiri koosneb sissejuhatusest, viiest peatükist ning kirjanduse loetelust, mis sisaldab 82 nimetust. Sissejuhatus kujutab endast esimest peatükki. Teises peatükis on toodud põhivõrrandid ning põhieeldused. Esimesed kaks peatükki on referatiivsed, ülejäänutes esitatakse originaalseid tulemusi. Kolmandas peatükis esitatakse nanotalade võnkumise võrrandid, mis arvestavad tala elementide pöördeinertsi. Need on Euler-Bernoulli võrrandite üldistuseks juhule, kui pöördeinertsi arvestamine on kohustuslik. See süsteem on lahendatav ka muutujate eraldamise teel. Neljandas peatükis lahendatakse põhivõrrandite süsteem numbriliselt. Näidatakse muuhulgas, et süsteemi saab hõlpsasti lahendada Maclaurini rea abil. Viies peatükk on pühendatud nanotalade võnkumise uurimisele juhul, kui nanotala on kinnitatud elastsete tugede abil st. toed ei ole jäigad.

Kuuendas peatükis uuritakse pragudega nanotalade võnkumisi arvestades termilisi mõjutusi st. temperatuuripingeid. Väitekirjas saadud tulemusi on võrreldud erijuhtudel kirjandusest leitavate tulemustega ning veendutud, et väitekirjas esitatud tulemused on heas kooskõlas teiste uurijate poolt saadud tulemustega. Väitekirjas saadud tulemuste põhjal on avaldatud koos juhendajaga 10 teadusartiklit.

ACKNOWLEDGEMENTS

First and foremost, I would like to express my gratitude to my supervisor, Prof. Jaan Lellep, who guided me throughout this project. His support and guidance were the main driving force to bring the project to reality. Importantly, I would like to offer my special thanks to Prof. Viktor Abramov, Prof. Arvet Pedas, and Prof. Rainis Haller for their advice during this course. I wish to show my appreciation to the secretaries at the Institute of Mathematics and Statistics for their help during this course. Nevertheless, I would like to acknowledge the ASTRA project where this research has been financed by the University of Tartu ASTRA Project PER ASPERA (European Regional Development Fund). Finally, I must express my very profound gratitude to my family members. None of this could have happened without their support.

PUBLICATIONS

CURRICULUM VITAE

Personal Data

Name:	Mohammed Mainul Hossain
Address:	Institute of Mathematics and Statistics, University of Tartu, Estonia.
Nationality:	Bangladesh.
Phone:	+372 56702638
Email:	mainul.hossain@ut.ee, mainul@mail.ee

Education

2022	Doctor of Philosophy in Mathematics, University of Tartu, Estonia
2015	Master of Philosophy in Mathematics, Bangladesh University of Engineering and Technology, Bangladesh.

Employment

2021–2022	Junior Research Fellow, Institute of Mathematics and Statistics, Tartu, Estonia.
2012–2018	Computer Programmer, Ecotech Group, Bangladesh.

Professional Training

2020–2021	Java Programming, Software Development Academy, Poland.

Scientific work

Publication in journals

1. Hossain, Mainul; Lellep, Jaan (2021). Transverse vibration of tapered nanobeam with elastic supports. Engineering Research Express, 3 (1), 015019. DOI: 10.1088 /2631-8695/abe10a.
2. Hossain, M.; Lellep, J. (2021). Natural vibrations of nanostrips with cracks. Acta Universitatis Tartuensis, 25 (1), 87105. DOI: 10.12697/ACUTM.2021.25.06.
3. Hossain,Mainul;Lellep,Jaan; (2021). Thermo mechanical vibration of single wall carbon nanotube partially embedded into soil medium. Agronomy Research, 19 (1), 777787. DOI: 10.15159/AR.21.027.
4. Hossain, M.M.; Lellep, J. (2021). Mode shape analysis of dynamic behaviour of cracked nanobeam on elastic foundation. Engineering Research Express, 3 (4). DOI: 10.1088/2631-8695/ac2a75.
5. Hossain, Mainul; Lellep, Jaan (2020). The effect of rotatory inertia on natural

frequency of cracked and stepped nanobeam. Engineering Research Express, 2 (3), 035009. DOI: 10.1088/2631-8695/aba48b.
6. Mainul Hossain and Jaan Lellep, Analysis of free vibration of tapered cracked double nanobeams using Maclaurin series, Eng. Res. Express, 4(2), 025034 (2022).
7. Mainul Hossain and Jaan Lellep, Natural vibration of axially graded multi cracked nanobeams in thermal environment using power series, J. Vib. Eng. Technol., (2022), "https://doi.org/10.1007/s42417-022-00555-3".

Publication in proceedings

1. Hossain, Mainul; Lellep, Jaan (2020). Effect of temperature on dynamic behavior of cracked metallic and composite beam. Vibroengineering Procedia, 32, 172178. DOI: 10.21595/vp.2020.21337.
2. Lellep, Jaan ; Hossain, Mainul (2019). Free vibrations of rectangular nanoplate strips. In: Juozapaitis, Algirdas; Daniūnas, Alfonsas; Juknevičius, Linas (Ed.). The proceedings of the 13th international conference (MBMST 2019) (743749). Vilnius: VGTU Press Technika. DOI: 10.3846/mbmst.2019.026.
3. Hossain, M; Lellep, J (2019). Natural vibration of stepped nanoplate with crack on an elastic foundation. IOP Conference Series Materials Science and Engineering, 660, 012051. DOI: 10.1088/1757-899X/660/1/012051.
4. M. Mainul Hossain, M. A. H. Khan, “Stability of MHD wall driven flow through a tube”, Procedia Engineering, Volume 194, 2017, Pages 428-434.
5. M. Mainul Hossain, M. A. H. Khan, “Stability analysis of wall driven nanofluid flow through a tube”, AIP Conference Proceedings 1851, 020024, (2017).
6. M. Mainul Hossain, “Stability of injected flow through a porous tube with magnetic field”, AIP Conference Proceedings, 1980, 040005 (2018).

Conferences

1. 13th International Conference "Modern Building Materials, Structures and Techniques" Vilnius, Lithuania, 16-17 of May 2019.
2. 4th International Conference “Innovative Materials, Structures and Technologies”, Riga, Latvia, 25-27 September 2019.
3. 46th International JVE Conference, 2020 in St. Petersburg, Russia, June 29 - July 1 2020.
4. Biosystems Engineering 2021, University of life science, Tartu, Estonia, 5-7 May, 2021.

ELULOOKIRJELDUS

Isikuandmed

Nimi:	Mohammed Mainul Hossain
Aadress:	Institute of Mathematics and Statistics, University of Tartu, Estonia.
Rahvus:	Bangladesh.
Telefon:	+372 56702638
E-post:	mainul.hossain@ut.ee, mainul@mail.ee

Haridus

2022	Doctor of Philosophy in Mathematics, University of Tartu, Estonia
2015	Master of Philosophy in Mathematics, Bangladesh University of Engineering and Technology, Bangladesh.

Teenistuskäik

2021–2022	Junior Research Fellow, Institute of Mathematics and Statistics, Tartu, Estonia.
2012–2018	Computer Programmer, Ecotech Group, Bangladesh.

Professionaalne treening

2020–2021	Java Programming, Software Development Academy, Poland.

Teadustegevus

Ajakirjades avaldamine

1. Hossain, Mainul; Lellep, Jaan (2021). Transverse vibration of tapered nanobeam with elastic supports. Engineering Research Express, 3 (1), 015019. DOI: 10.1088/2631-8695/abe10a.
2. Hossain, M.; Lellep, J. (2021). Natural vibrations of nanostrips with cracks. Acta Universitatis Tartuensis, 25 (1), 87105. DOI: 10.12697/ACUTM.2021.25.06.
3. Hossain,Mainul;Lellep,Jaan; (2021). Thermo mechanical vibration of single wall carbon nanotube partially embedded into soil medium. Agronomy Research, 19 (1), 777787. DOI: 10.15159/AR.21.027.
4. Hossain, M.M.; Lellep, J. (2021). Mode shape analysis of dynamic behaviour of cracked nanobeam on elastic foundation. Engineering Research Express, 3 (4). DOI: 10.1088/2631-8695/ac2a75.
5. Hossain, Mainul; Lellep, Jaan (2020). The effect of rotatory inertia on natural

frequency of cracked and stepped nanobeam. Engineering Research Express, 2 (3), 035009. DOI: 10.1088/2631-8695/aba48b.
6. Mainul Hossain and Jaan Lellep, Analysis of free vibration of tapered cracked double nanobeams using Maclaurin series, Eng. Res. Express, 4(2), 025034 (2022).
7. Mainul Hossain and Jaan Lellep, Natural vibration of axially graded multi cracked nanobeams in thermal environment using power series, J. Vib. Eng. Technol., (2022), "https://doi.org/10.1007/s42417-022-00555-3".

Avaldamine menetluses

1. Hossain, Mainul; Lellep, Jaan (2020). Effect of temperature on dynamic behavior of cracked metallic and composite beam. Vibroengineering Procedia, 32, 172178. DOI: 10.21595/vp.2020.21337.
2. Lellep, Jaan ; Hossain, Mainul (2019). Free vibrations of rectangular nanoplate strips. In: Juozapaitis, Algirdas; Daniūnas, Alfonsas; Juknevičius, Linas (Ed.). The proceedings of the 13th international conference (MBMST 2019) (743749). Vilnius: VGTU Press Technika. DOI: 10.3846/mbmst.2019.026.
3. Hossain, M; Lellep, J (2019). Natural vibration of stepped nanoplate with crack on an elastic foundation. IOP Conference Series Materials Science and Engineering, 660, 012051. DOI: 10.1088/1757-899X/660/1/012051.
4. M. Mainul Hossain, M. A. H. Khan, “Stability of MHD wall driven flow through a tube”, Procedia Engineering, Volume 194, 2017, Pages 428-434.
5. M. Mainul Hossain, M. A. H. Khan, “Stability analysis of wall driven nanofluid flow through a tube”, AIP Conference Proceedings 1851, 020024, (2017).
6. M. Mainul Hossain, “Stability of injected flow through a porous tube with magnetic field”, AIP Conference Proceedings, 1980, 040005 (2018).

Konverentsid

1. 13th International Conference "Modern Building Materials, Structures and Techniques"Vilnius, Lithuania, 16-17 of May 2019.
2. 4th International Conference “Innovative Materials, Structures and Technologies”, Riga, Latvia, 25-27 September 2019.
3. 46th International JVE Conference, 2020 in St. Petersburg, Russia, June 29 - July 1 2020.
4. Biosystems Engineering 2021, University of life science, Tartu, Estonia, 5-7 May, 2021.

DISSERTATIONES MATHEMATICAE UNIVERSITATIS TARTUENSIS

1. **Mati Heinloo.** The design of nonhomogeneous spherical vessels, cylindrical tubes and circular discs. Tartu, 1991, 23 p.
2. **Boris Komrakov.** Primitive actions and the Sophus Lie problem. Tartu, 1991, 14 p.
3. **Jaak Heinloo.** Phenomenological (continuum) theory of turbulence. Tartu, 1992, 47 p.
4. **Ants Tauts.** Infinite formulae in intuitionistic logic of higher order. Tartu, 1992, 15 p.
5. **Tarmo Soomere.** Kinetic theory of Rossby waves. Tartu, 1992, 32 p.
6. **Jüri Majak.** Optimization of plastic axisymmetric plates and shells in the case of Von Mises yield condition. Tartu, 1992, 32 p.
7. **Ants Aasma.** Matrix transformations of summability and absolute summability fields of matrix methods. Tartu, 1993, 32 p.
8. **Helle Hein.** Optimization of plastic axisymmetric plates and shells with piece-wise constant thickness. Tartu, 1993, 28 p.
9. **Toomas Kiho.** Study of optimality of iterated Lavrentiev method and its generalizations. Tartu, 1994, 23 p.
10. **Arne Kokk.** Joint spectral theory and extension of non-trivial multiplicative linear functionals. Tartu, 1995, 165 p.
11. **Toomas Lepikult.** Automated calculation of dynamically loaded rigid-plastic structures. Tartu, 1995, 93 p, (in Russian).
12. **Sander Hannus.** Parametrical optimization of the plastic cylindrical shells by taking into account geometrical and physical nonlinearities. Tartu, 1995, 74 p, (in Russian).
13. **Sergei Tupailo.** Hilbert's epsilon-symbol in predicative subsystems of analysis. Tartu, 1996, 134 p.
14. **Enno Saks.** Analysis and optimization of elastic-plastic shafts in torsion. Tartu, 1996, 96 p.
15. **Valdis Laan.** Pullbacks and flatness properties of acts. Tartu, 1999, 90 p.
16. **Märt Põldvere.** Subspaces of Banach spaces having Phelps' uniqueness property. Tartu, 1999, 74 p.
17. **Jelena Ausekle.** Compactness of operators in Lorentz and Orlicz sequence spaces. Tartu, 1999, 72 p.
18. **Krista Fischer.** Structural mean models for analyzing the effect of compliance in clinical trials. Tartu, 1999, 124 p.
19. **Helger Lipmaa.** Secure and efficient time-stamping systems. Tartu, 1999, 56 p.
20. **Jüri Lember.** Consistency of empirical k-centres. Tartu, 1999, 148 p.
21. **Ella Puman.** Optimization of plastic conical shells. Tartu, 2000, 102 p.
22. **Kaili Müürisep.** Eesti keele arvutigrammatika: süntaks. Tartu, 2000, 107 lk.

23. **Varmo Vene.** Categorical programming with inductive and coinductive types. Tartu, 2000, 116 p.
24. **Olga Sokratova.** Ω-rings, their flat and projective acts with some applications. Tartu, 2000, 120 p.
25. **Maria Zeltser.** Investigation of double sequence spaces by soft and hard analitical methods. Tartu, 2001, 154 p.
26. **Ernst Tungel.** Optimization of plastic spherical shells. Tartu, 2001, 90 p.
27. **Tiina Puolakainen.** Eesti keele arvutigrammatika: morfoloogiline ühestamine. Tartu, 2001, 138 p.
28. **Rainis Haller.** *M(r,s)*-inequalities. Tartu, 2002, 78 p.
29. **Jan Villemson.** Size-efficient interval time stamps. Tartu, 2002, 82 p.
30. Töö kaitsmata.
31. **Mart Abel.** Structure of Gelfand-Mazur algebras. Tartu, 2003. 94 p.
32. **Vladimir Kuchmei.** Affine completeness of some ockham algebras. Tartu, 2003. 100 p.
33. **Olga Dunajeva.** Asymptotic matrix methods in statistical inference problems. Tartu 2003. 78 p.
34. **Mare Tarang.** Stability of the spline collocation method for volterra integro-differential equations. Tartu 2004. 90 p.
35. **Tatjana Nahtman.** Permutation invariance and reparameterizations in linear models. Tartu 2004. 91 p.
36. **Märt Möls.** Linear mixed models with equivalent predictors. Tartu 2004. 70 p.
37. **Kristiina Hakk.** Approximation methods for weakly singular integral equations with discontinuous coefficients. Tartu 2004, 137 p.
38. **Meelis Käärik.** Fitting sets to probability distributions. Tartu 2005, 90 p.
39. **Inga Parts.** Piecewise polynomial collocation methods for solving weakly singular integro-differential equations. Tartu 2005, 140 p.
40. **Natalia Saealle.** Convergence and summability with speed of functional series. Tartu 2005, 91 p.
41. **Tanel Kaart.** The reliability of linear mixed models in genetic studies. Tartu 2006, 124 p.
42. **Kadre Torn.** Shear and bending response of inelastic structures to dynamic load. Tartu 2006, 142 p.
43. **Kristel Mikkor.** Uniform factorisation for compact subsets of Banach spaces of operators. Tartu 2006, 72 p.
44. **Darja Saveljeva.** Quadratic and cubic spline collocation for Volterra integral equations. Tartu 2006, 117 p.
45. **Kristo Heero.** Path planning and learning strategies for mobile robots in dynamic partially unknown environments. Tartu 2006, 123 p.
46. **Annely Mürk.** Optimization of inelastic plates with cracks. Tartu 2006. 137 p.
47. **Annemai Raidjõe.** Sequence spaces defined by modulus functions and superposition operators. Tartu 2006, 97 p.
48. **Olga Panova.** Real Gelfand-Mazur algebras. Tartu 2006, 82 p.

49. **Härmel Nestra.** Iteratively defined transfinite trace semantics and program slicing with respect to them. Tartu 2006, 116 p.
50. **Margus Pihlak.** Approximation of multivariate distribution functions. Tartu 2007, 82 p.
51. **Ene Käärik.** Handling dropouts in repeated measurements using copulas. Tartu 2007, 99 p.
52. **Artur Sepp.** Affine models in mathematical finance: an analytical approach. Tartu 2007, 147 p.
53. **Marina Issakova.** Solving of linear equations, linear inequalities and systems of linear equations in interactive learning environment. Tartu 2007, 170 p.
54. **Kaja Sõstra.** Restriction estimator for domains. Tartu 2007, 104 p.
55. **Kaarel Kaljurand.** Attempto controlled English as a Semantic Web language. Tartu 2007, 162 p.
56. **Mart Anton.** Mechanical modeling of IPMC actuators at large deformations. Tartu 2008, 123 p.
57. **Evely Leetma.** Solution of smoothing problems with obstacles. Tartu 2009, 81 p.
58. **Ants Kaasik.** Estimating ruin probabilities in the Cramér-Lundberg model with heavy-tailed claims. Tartu 2009, 139 p.
59. **Reimo Palm.** Numerical Comparison of Regularization Algorithms for Solving Ill-Posed Problems. Tartu 2010, 105 p.
60. **Indrek Zolk.** The commuting bounded approximation property of Banach spaces. Tartu 2010, 107 p.
61. **Jüri Reimand.** Functional analysis of gene lists, networks and regulatory systems. Tartu 2010, 153 p.
62. **Ahti Peder.** Superpositional Graphs and Finding the Description of Structure by Counting Method. Tartu 2010, 87 p.
63. **Marek Kolk.** Piecewise Polynomial Collocation for Volterra Integral Equations with Singularities. Tartu 2010, 134 p.
64. **Vesal Vojdani.** Static Data Race Analysis of Heap-Manipulating C Programs. Tartu 2010, 137 p.
65. **Larissa Roots.** Free vibrations of stepped cylindrical shells containing cracks. Tartu 2010, 94 p.
66. **Mark Fišel.** Optimizing Statistical Machine Translation via Input Modification. Tartu 2011, 104 p.
67. **Margus Niitsoo**. Black-box Oracle Separation Techniques with Applications in Time-stamping. Tartu 2011, 174 p.
68. **Olga Liivapuu.** Graded q-differential algebras and algebraic models in noncommutative geometry. Tartu 2011, 112 p.
69. **Aleksei Lissitsin.** Convex approximation properties of Banach spaces. Tartu 2011, 107 p.
70. **Lauri Tart.** Morita equivalence of partially ordered semigroups. Tartu 2011, 101 p.
71. **Siim Karus.** Maintainability of XML Transformations. Tartu 2011, 142 p.

72. **Margus Treumuth.** A Framework for Asynchronous Dialogue Systems: Concepts, Issues and Design Aspects. Tartu 2011, 95 p.
73. **Dmitri Lepp.** Solving simplification problems in the domain of exponents, monomials and polynomials in interactive learning environment T-algebra. Tartu 2011, 202 p.
74. **Meelis Kull.** Statistical enrichment analysis in algorithms for studying gene regulation. Tartu 2011, 151 p.
75. **Nadežda Bazunova.** Differential calculus $d^3 = 0$ on binary and ternary associative algebras. Tartu 2011, 99 p.
76. **Natalja Lepik.** Estimation of domains under restrictions built upon generalized regression and synthetic estimators. Tartu 2011, 133 p.
77. **Bingsheng Zhang.** Efficient cryptographic protocols for secure and private remote databases. Tartu 2011, 206 p.
78. **Reina Uba.** Merging business process models. Tartu 2011, 166 p.
79. **Uuno Puus.** Structural performance as a success factor in software development projects – Estonian experience. Tartu 2012, 106 p.
80. **Marje Johanson.** $M(r, s)$-ideals of compact operators. Tartu 2012, 103 p.
81. **Georg Singer.** Web search engines and complex information needs. Tartu 2012, 218 p.
82. **Vitali Retšnoi.** Vector fields and Lie group representations. Tartu 2012, 108 p.
83. **Dan Bogdanov.** Sharemind: programmable secure computations with practical applications. Tartu 2013, 191 p.
84. **Jevgeni Kabanov.** Towards a more productive Java EE ecosystem. Tartu 2013, 151 p.
85. **Erge Ideon**. Rational spline collocation for boundary value problems. Tartu, 2013, 111 p.
86. **Esta Kägo.** Natural vibrations of elastic stepped plates with cracks. Tartu, 2013, 114 p.
87. **Margus Freudenthal.** Simpl: A toolkit for Domain-Specific Language development in enterprise information systems. Tartu, 2013, 151 p.
88. **Boriss Vlassov.** Optimization of stepped plates in the case of smooth yield surfaces. Tartu, 2013, 104 p.
89. **Elina Safiulina.** Parallel and semiparallel space-like submanifolds of low dimension in pseudo-Euclidean space. Tartu, 2013, 85 p.
90. **Raivo Kolde.** Methods for re-using public gene expression data. Tartu, 2014, 121 p.
91. **Vladimir Šor.** Statistical Approach for Memory Leak Detection in Java Applications. Tartu, 2014, 155 p.
92. **Naved Ahmed.** Deriving Security Requirements from Business Process Models. Tartu, 2014, 171 p.
93. **Kerli Orav-Puurand.** Central Part Interpolation Schemes for Weakly Singular Integral Equations. Tartu, 2014, 109 p.
94. **Liina Kamm.** Privacy-preserving statistical analysis using secure multi-party computation. Tartu, 2015, 201 p.

95. **Kaido Lätt.** Singular fractional differential equations and cordial Volterra integral operators. Tartu, 2015, 93 p.
96. **Oleg Košik.** Categorical equivalence in algebra. Tartu, 2015, 84 p.
97. **Kati Ain.** Compactness and null sequences defined by ℓ_p spaces. Tartu, 2015, 90 p.
98. **Helle Hallik.** Rational spline histopolation. Tartu, 2015, 100 p.
99. **Johann Langemets.** Geometrical structure in diameter 2 Banach spaces. Tartu, 2015, 132 p.
100. **Abel Armas Cervantes.** Diagnosing Behavioral Differences between Business Process Models. Tartu, 2015, 193 p.
101. **Fredrik Milani.** On Sub-Processes, Process Variation and their Interplay: An Integrated Divide-and-Conquer Method for Modeling Business Processes with Variation. Tartu, 2015, 164 p.
102. **Huber Raul Flores Macario.** Service-Oriented and Evidence-aware Mobile Cloud Computing. Tartu, 2015, 163 p.
103. **Tauno Metsalu.** Statistical analysis of multivariate data in bioinformatics. Tartu, 2016, 197 p.
104. **Riivo Talviste.** Applying Secure Multi-party Computation in Practice. Tartu, 2016, 144 p.
105. **Md Raknuzzaman.** Noncommutative Galois Extension Approach to Ternary Grassmann Algebra and Graded q-Differential Algebra. Tartu, 2016, 110 p.
106. **Alexander Liyvapuu.** Natural vibrations of elastic stepped arches with cracks. Tartu, 2016, 110 p.
107. **Julia Polikarpus.** Elastic plastic analysis and optimization of axisymmetric plates. Tartu, 2016, 114 p.
108. **Siim Orasmaa.** Explorations of the Problem of Broad-coverage and General Domain Event Analysis: The Estonian Experience. Tartu, 2016, 186 p.
109. **Prastudy Mungkas Fauzi.** Efficient Non-interactive Zero-knowledge Protocols in the CRS Model. Tartu, 2017, 193 p.
110. **Pelle Jakovits.** Adapting Scientific Computing Algorithms to Distributed Computing Frameworks. Tartu, 2017, 168 p.
111. **Anna Leontjeva.** Using Generative Models to Combine Static and Sequential Features for Classification. Tartu, 2017, 167 p.
112. **Mozhgan Pourmoradnasseri.** Some Problems Related to Extensions of Polytopes. Tartu, 2017, 168 p.
113. **Jaak Randmets.** Programming Languages for Secure Multi-party Computation Application Development. Tartu, 2017, 172 p.
114. **Alisa Pankova.** Efficient Multiparty Computation Secure against Covert and Active Adversaries. Tartu, 2017, 316 p.
115. **Tiina Kraav.** Stability of elastic stepped beams with cracks. Tartu, 2017, 126 p.
116. **Toomas Saarsen.** On the Structure and Use of Process Models and Their Interplay. Tartu, 2017, 123 p.

117. **Silja Veidenberg.** Lifting bounded approximation properties from Banach spaces to their dual spaces. Tartu, 2017, 112 p.
118. **Liivika Tee.** Stochastic Chain-Ladder Methods in Non-Life Insurance. Tartu, 2017, 110 p.
119. **Ülo Reimaa.** Non-unital Morita equivalence in a bicategorical setting. Tartu, 2017, 86 p.
120. **Rauni Lillemets.** Generating Systems of Sets and Sequences. Tartu, 2017, 181 p.
121. **Kristjan Korjus.** Analyzing EEG Data and Improving Data Partitioning for Machine Learning Algorithms. Tartu, 2017, 106 p.
122. **Eno Tõnisson.** Differences between Expected Answers and the Answers Offered by Computer Algebra Systems to School Mathematics Equations. Tartu, 2017, 195 p.
123. **Kaur Lumiste.** Improving accuracy of survey estimators by using auxiliary information in data collection and estimation stages. Tartu, 2018, 112 p.
124. **Paul Tammo.** Closed maximal regular one-sided ideals in topological algebras. Tartu, 2018, 112 p.
125. **Mart Kals.** Computational and statistical methods for DNA sequencing data analysis and applications in the Estonian Biobank cohort. Tartu, 2018, 174 p.
126. **Annika Krutto.** Empirical Cumulant Function Based Parameter Estimation in Stable Distributions. Tartu, 2019, 140 p.
127. **Kristi Läll.** Risk scores and their predictive ability for common complex diseases. Tartu, 2019, 118 p.
128. **Gul Wali Shah.** Spline approximations. Tartu, 2019, 85 p.
129. **Mikk Vikerpuur.** Numerical solution of fractional differential equations. Tartu, 2019, 125 p.
130. **Priit Lätt.** Induced 3-Lie superalgebras and their applications in superspace. Tartu, 2020, 114 p.
131. **Sumaira Rehman.** Fast and quasi-fast solvers for weakly singular Fredholm integral equation of the second kind. Tartu, 2020, 105 p.
132. **Rihhard Nadel.** Big slices of the unit ball in Banach spaces. Tartu, 2020, 109 p.
133. **Katriin Pirk.** Diametral diameter two properties, Daugavet-, and Δ-points in Banach spaces. Tartu, 2020, 106 p.
134. **Zahra Alijani**. Fuzzy integral equations of the second kind. Tartu, 2020, 103 1p.
135. **Hina Arif.** Stability analysis of stepped nanobeams with defects. Tartu, 2021, 165 p.
136. **Joonas Sova.** Pairwise Markov Models. Tartu, 2021, 166 p.
137. **Kristo Väljako.** On the Morita equivalence of idempotent rings and monomorphisms of firm bimodules. Tartu, 2022, 139 p.
138. **Andre Ostrak.** Diameter two properties in spaces of Lipschitz functions. Tartu, 2022, 77 p.